A Section 508–conformant HTML version of this article is available at https://doi.org/10.1289/EHP5862.

Role of TET Dioxygenases and DNA Hydroxymethylation in Bisphenols-Stimulated Proliferation of Breast Cancer Cells

Zhe Li,[1] Cong Lyu,[1,2] Yun Ren,[1,2] and Hailin Wang[1,2,3]

[1]State Key Laboratory of Environmental Chemistry and Ecotoxicology, Research Center for Eco-Environmental Sciences, Chinese Academy of Sciences, Beijing, China
[2]University of Chinese Academy of Sciences, Beijing, China
[3]Institute of Environment and Health, Jianghan University, Wuhan, China

Background: Bisphenol A (BPA), a ubiquitous environmental endocrine disruptor targeting estrogen receptors (ERs), has been implicated in the promotion of breast cancer. Perinatal exposure of BPA could induce longitudinal alteration of DNA hydroxymethylation in imprinted loci of mouse blood cells. To date, no data has been reported on the effects of BPA on DNA hydroxymethylation in breast cells. Therefore, we asked whether BPA can induce DNA hydroxymethylation change in human breast cells. Given that dysregulated epigenetic DNA hydroxymethylation is observed in various cancers, we wondered how DNA hydroxymethylation modulates cancer development, and specifically, whether and how BPA and its analogs promote breast cancer development via DNA hydroxymethylation.

Objectives: We aimed to explore the interplay of the estrogenic activity of bisphenols at environmental exposure dose levels with TET dioxygenase-catalyzed DNA hydroxymethylation and to elucidate their roles in the proliferation of ER^+ breast cancer cells as stimulated by environmentally relevant bisphenols.

Methods: Human MCF-7 and T47D cell lines were used as ER-dependent breast cell proliferation models, and the human MDA-MB-231 cell line was used as an ER-independent breast cell model. These cells were treated with BPA or bisphenol S (BPS) to examine BPA/BPS-related proliferation. Ultra-high performance liquid chromatography–tandem mass spectrometry (UHPLC-MS/MS) and enzyme-linked immunosorbent assays (ELISAs) were used to detect DNA hydroxymethylation. Crispr/Cas9 and RNA interference technologies, quantitative polymerase chain reaction (qPCR), and Western blot analyses were used to evaluate the expression and function of genes. Co-immunoprecipitation (Co-IP), bisulfite sequencing-PCR (BSP), and chromatin immunoprecipitation-qPCR (ChIP-qPCR) were used to identify the interactions of target proteins.

Results: We measured higher proliferation in ER^+ breast cancer cells treated with BPA or its replacement, BPS, accompanied by an ERα-dependent decrease in genomic DNA hydroxymethylation. The results of our overexpression, knockout, knockdown, and inhibition experiments suggested that TET2-catalyzed DNA hydroxymethylation played a suppressive role in BPA/BPS-stimulated cell proliferation. On the other hand, we observed that TET2 was negatively regulated by the activation of ERα (dimerized and phosphorylated), which was also induced by BPA/BPS binding. Instead of a direct interaction between TET2 and ERα, data of our Co-IP, BSP, and ChIP-qPCR experiments indicated that the activated ERα increased the DNA methyltransferase (DNMT)-mediated promoter methylation of TET2, leading to an inhibition of the TET2 expression and DNA hydroxymethylation.

Conclusions: We identified a new feedback circuit of ERα activation–DNMT-TET2-DNA hydroxymethylation in ER^+ breast cancer cells and uncovered a pivotal role of TET2-mediated DNA hydroxymethylation in modulating BPA/BPS-stimulated proliferation. Moreover, to our knowledge, we for the first time established a linkage among chemical exposure, DNA hydroxymethylation, and tumor-associated proliferation. These findings further clarify the estrogenic activity of BPA/BPS and its profound implications for the regulation of epigenetic DNA hydroxymethylation and cell proliferation. https://doi.org/10.1289/EHP5862

Introduction

Bisphenol A (BPA) is a well-known environmental endocrine disruptor, causing adverse alterations in the reproductive system, liver, and mammary glands (Vandenberg et al. 2007; Michałowicz 2014; Rodgers et al. 2018). In China, Canada, the United States, the European Union, and some other countries, BPA has been banned from use in the raw materials for the production of some baby products (EFSA CEF Panel 2015; Aungst 2014). Due to industrial demands, bisphenol S (BPS) has been widely used as a replacement for BPA in the production of thermal paper, food packaging materials, food can coatings, and bottles and in leather processing (Chen et al. 2016; Rochester and Bolden 2015). Recent studies demonstrated that BPS also has estrogenic activity (Chen et al. 2016; Héliès-Toussaint et al. 2014; Kinch et al. 2015; Viñas and Watson 2013).

Environmental exposures of BPA and BPS to humans have been extensively surveyed. Both BPA ($n_{BPA} = 293$, 93%) (Zhang et al. 2011) and BPS ($n_{BPS} = 255$, 81%) (Liao et al. 2012) were detected in most urine samples ($n_{total} = 315$) from the United States and seven Asian countries. Epidemiological surveys in the United States showed that BPA levels (ranging from 0.4 to 149 μg/L) were detectable in 95% of the urine samples (Calafat et al. 2005; Zhou et al. 2014), and biomonitoring studies indicated that BPA was also found in maternal plasma (3.1 ng/mL; ∼13 nM), fetal plasma (2.3 ng/mL; ∼10 nM), amniotic fluid (8 ng/mL; ∼35 nM), and placental tissues (1–104.9 ng/g) (Corrales et al. 2015; Pfeifer et al. 2015; Vandenberg et al. 2010).

The endogenous hormone estradiol (E_2) is a key regulator for a variety of physiological functions and acts through two estrogen receptors (ERs), ERα and ERβ (Burns et al. 2011; Pettersson and Gustafsson 2001). The adverse health effects of BPA and BPS might be associated with their ability to regulate the actions of ERs (Acconcia et al. 2015; Viñas and Watson 2013). To explain BPA-caused dysregulation of gene transcription and health effects, three major ER-associated mechanisms have been proposed: *a*) direct interaction of the ligand-bound ER with DNA estrogen response elements (EREs) that are located in the regulatory regions of the ER target genes (Pettersson and Gustafsson 2001); *b*) interaction of the ERs with other transcription factors (TFs), such as activator protein 1 (AP-1) or Sp1 transcription factor (SP-1) (Métivier et al. 2003); and *c*) activation of intracellular signaling cascades involving p44/42, mitogen-activated protein kinase (MAPK), SRC proto-oncogene, non-receptor tyrosine kinase (Src), and AKT serine/threonine kinase 1 (Akt) (Burns et al. 2011). However, epigenetic factors involved

Address correspondence to Hailin Wang, Research Center for Eco-Environmental Sciences, Chinese Academy of Sciences, P.O. Box 2871, Beijing 100085 China. Telephone: 86-10-62849600. Email: hlwang@rcees.ac.cn

Supplemental Material is available online (https://doi.org/10.1289/EHP5862).
The authors declare they have no actual or potential competing financial interests.
Received 9 July 2019; Revised 31 January 2020; Accepted 5 February 2020; Published 27 February 2020.

in those mechanisms remain unclear. We attempted to gain new insight into the BPA/BPS-caused health effects via epigenetic DNA hydroxymethylation.

DNA 5-hydroxymethylcytosine (5hmC) is a major oxidation product of DNA 5-methylcytosine (5mC) catalyzed by the ten-eleven translocation (TET) family of dioxygenases (Tahiliani et al. 2009) and is critical for active and passive DNA demethylation (He et al. 2011), locus-specific regulation of gene activities (Wu and Zhang 2010), and large-scale nuclear reprograming (Ficz et al. 2011; Tan and Shi 2012). The alterations in genomic 5hmC and TET dioxygenases are tightly associated with the survival rate of cancer patients (Haffner et al. 2011; Jin et al. 2011; Tan and Shi 2012) and involved with breast (Zhong et al. 2019), prostate, liver (Liu et al. 2019), lung, pancreatic, colorectal, gastric, small intestine, brain, kidney, and skin cancers and myeloid diseases (Albano et al. 2011; Chou et al. 2011; Ko et al. 2010). At the global level, genomic 5hmC has been shown to be much more dramatically decreased in the cancer state than in normal tissue compared with genomic 5mC (Haffner et al. 2011; Tan and Shi 2012). Interestingly, perinatal exposure of BPA can induce persistent 5hmC markers at imprinted loci in mouse blood throughout development (Kochmanski et al. 2018).

As a stable epigenetic marker in mammalian tissues, 5hmC is a better indicator of stimuli of environmental molecules than the well-known 5mC marker (Yin et al. 2013; Zhao et al. 2014, Zhong et al. 2019). We wondered if BPA and BPS could induce alteration of the 5hmC marker. That perinatal BPA exposure has resulted in a change of the 5hmC loci in mouse blood (Kochmanski et al. 2018) supports this probability. So the question was whether and how DNA hydroxymethylation shapes the adverse health effects caused by BPA/BPS exposure, especially cellular proliferation. Of note, cellular proliferation is a critical indicator for the growth, invasion, recurrence, and metastasis of cancers (López-Sáez et al. 1998; Zhu and Thompson 2019). To answer our questions, we explored the interplay between estrogenic activity, TET dioxygenases, and 5hmC and investigated their roles in the proliferation of breast cancer cells upon BPA/BPS exposure.

Materials and Methods

Chemicals and Antibodies

Dimethyl sulfoxide (DMSO), 17-beta-estradiol (E_2), BPA, and BPS were obtained from Sigma Chemical Co. Dimethyloxaloylglycine (DMOG) was purchased from Absin. Antibodies used in this work are listed in the Table S1.

Cell Culture

Human breast cancer cell lines MCF-7 (ER^+, with higher ERα/ERβ ratios), T47D (ER^+, with lower ERα/ERβ ratios), and MDA-MB-231 (a triple-negative breast cancer cell line) were supplied by the cell culture center of the Chinese Academy of Medical Sciences. MCF-7 and MDA-MB-231 cells were cultured in phenol red-free Dulbecco's modified Eagle's medium (DMEM) supplemented with a high-glucose medium containing charcoal-stripped fetal bovine serum (FBS; Catalog No. 12676011, GIBCO, New Zealand Origin), 1% glutamine, and 1% penicillin/streptomycin. T47D was cultured in phenol red-free RPMI 1640 medium supplemented with 10% charcoal-stripped FBS, 1% glutamine, and 1% penicillin/streptomycin. All cell lines were incubated in 5% carbon dioxide (CO_2) at 37°C.

Justified Doses of BPA and BPS Treatment

Based on more than 80 published human biomonitoring studies, long-term exposure of BPA leads to steady-state BPA concentrations in the nanograms-per-milliliter (nanomolar) range in human urine and blood (Calafat et al. 2005; Vandenberg et al. 2010; Zhou et al. 2014). Vandenberg et al. (2007) estimated the theoretical internal dose to be 10–100 nM among the general population, based on measured levels of BPA in body fluids and tissues. Therefore, the environmentally relevant doses of BPA/BPS (10–1,000 nM) were chosen for use in our study.

Cell Treatment with BPA or BPS

BPA and BPS were each dissolved in DMSO, and a 20-mM stock solution of each was stored at room temperature (RT) and diluted as needed to the indicated concentrations using culture medium. The final DMSO concentration in the culture medium was 0.1% (vol/vol). Medium with 0.1% (vol/vol) DMSO (vehicle) was used as the control. Three wells per assay were used for each treatment in each cell line.

MCF-7, T47D, and MDA-MB-231 cells were cultured in 96-well plates or 6-cm dishes for 24 h and then treated with 10–1,000 nM BPA/BPS for 24, 48, or 72 h, after which the cells were harvested for cell proliferation assays or for 5hmC analysis. MCF-7 cells were cultured in 6-cm dishes for 24 h and then treated with 10–1,000 nM BPA/BPS for 24, 48, and 72 h, after which the cells were used for DNA or RNA extraction, enzyme-linked immunosorbent assays (ELISAs), bisulfite sequencing, protein extraction, plasmid transfection, and subsequent experiments. MCF-7 cells were cultured in eight-chamber slides (Lab-tek) for 24 h and then treated with 10–1,000 nM BPA/BPS for 24, 48, and 72 h, after which the cells were used for immunofluorescent staining and imaging analysis.

Cell Treatment with E_2

E_2 was dissolved in DMSO to a stock solution of 10 mM. The stock solution was diluted as needed to the indicated concentrations using culture medium.

MCF-7 cells were cultured in 96-well plates for 24 h and then treated with 1.0 nM E_2 for 24, 48, or 72 h, after which the cells were used for cell proliferation assays. Similarly, MCF-7 cells were cultured in 6-cm dishes for DNA or RNA extraction, 5hmC analysis, protein extraction, and subsequent experiments. Three wells per assay were used for each treatment.

Cell Treatment with DMOG

MCF-7 cells were treated with 200 mM DMOG for 24 h. The cells were then subjected to BPA and BPS exposure, as described for proliferation and for 5hmC analysis.

MTS Cell Proliferation Assay

The MTS assay is based on the conversion of a tetrazolium salt [3-(4,5-dimethylthiazol-2-yl)-5-(3-carboxymethoxyphenyl)-2-(4-sulfophenyl)-2H-tetrazolium] into a colored, aqueous-soluble formazan product by mitochondrial activity (Malich et al. 1997). We used a cell density of 2×10^3 cells (MCF-7, T47D, and MDA-MB-231 cells) per well as a starting point. After culture in 96-well plates for 24 h, the cells were exposed to BPA, BPS, or vehicle at different concentrations. At the indicated times, the cells were incubated with the MTS assay reagents for 4 h, and absorbance was measured at 490 nm by a microplate reader (Varioskan Flash, Thermo).

The relative proliferation was calculated by the formula: $[A_{(sample)} - A_{(blank)}]/A_{(blank)}$. $A_{(sample)}$ represented the optical density $(OD)_{490}$ value of cells treated with vehicle, BPA, or BPS, and $A_{(blank)}$ represented the OD_{490} value of the blank group. Note, the blank group contained only culture medium and MTS solution (without cells).

5-Ethynyl-2′-Deoxyuridine Cell Proliferation Assay

After being seeded (5,000 cells per chamber) in eight-chamber slides (Lab-tek) for 24 h, MCF-7 cells were treated with BPA or BPS at different concentrations. At indicated times, cells were incubated with 5-ethynyl-2′-deoxyuridine (EdU; 30 μM) from Invitrogen for 6 h and then washed twice with phosphate-buffered saline (PBS; Catalog No. 10010049, Gibco, Thermo Scientific) and fixed with 4% paraformaldehyde for 10 min. MCF-7 cells were permeabilized with 0.1% Triton X-100 in PBS for 5 min, then incubated with 5% normal donkey serum–blocking buffer for 2 h. Incorporated EdU was detected with a copper-catalyzed fluorescent azide reaction (Click-iT EdU Microplate Assay, Catalog No. C10214, Invitrogen), after which the slides were washed with PBS and mounted on cover slips with mounting medium containing 4′,6-diamidino-2-phenylindole (DAPI) (Vector). Fluorescence imaging was collected by confocal fluorescence microscopy (Leica). The EdU signal was visualized with excitation at 550 nm and emission at 565 nm, and the DAPI signal was visualized with excitation at 350 nm and emission at 461 nm.

DNA Extraction and Enzymatic Digestion

Following our previous work (Yin et al. 2013; Zhao et al. 2014), genomic DNA was extracted from the harvested cells (MCF-7, T47D, and MDA-MB-231 cells) using a Genomic DNA Purification Kit (Promega) according to the manufacturer's instructions. The DNA (5 μg) was digested to nucleosides with 1.0 U DNase I, 2.0 U calf intestinal phosphatase, and 0.005 U snake venom phosphodiesterase I (New England Biolabs) at 37°C for 24 h. The digests were filtered using ultrafiltration tubes (Millipore) by centrifuging at $10{,}000 \times g$ for 30 min in order to remove the proteins from the DNA digestion system.

Ultra-High Performance Liquid Chromatography–Tandem Mass Spectrometry Analysis

The digested DNA (5.0–15.0 μL) was subjected to ultra-high performance liquid chromatography–tandem mass spectrometry (UHPLC-MS/MS) analysis for detection of 5hmC and 5mC, as previously described (Yin et al. 2013; Zhao et al. 2014). The Agilent 1200 Series Rapid Resolution LC system with a reverse-phase Zorbax SB-C18 2.1×100 mm column (1.8-mm particles) was applied for UHPLC separation. Mass spectrometric detection in the positive ion mode was achieved by the Agilent 6410B triple quadrupole MS with an electrospray ionization source.

Quantification of Global DNA Hydroxymethylation (5hmC) by ELISA

The extracted genomic DNA was stored at −80°C. Global DNA hydroxymethylation (5hmC) were assessed using the MethylFlash Global DNA Hydroxymethylation ELISA Easy kit (colorimetric) from EpiGentek.

Immunofluorescent Staining And Imaging Analysis

Cultured MCF-7 cells (5,000 cells per chamber) were plated onto eight-chamber slides (Lab-tek) and treated with 10–1,000 nM BPA/BPS for 48 h. At the indicated times, the MCF-7 cells were first washed with PBS and then fixed with 4% paraformaldehyde solution for 15 min, followed by another PBS wash. After permeabilization with 0.1% Triton X-100 in PBS for 10 min, the MCF-7 cells were incubated with 4 N HCl for 15 min at RT, rinsed with distilled water, and placed in 100 mM Tris–HCl (pH 8.5) for 10 min. The MCF-7 cells were washed with PBS and incubated in a blocking solution [3% goat serum in PBS-Tween (PBST; Catalog No. 28352, Pierce, Thermo Scientific)] for 1 h at RT. The MCF-7 cells were then treated with diluted (1:1,000) anti-5hmC rabbit polyclonal antibody (Active Motif) overnight at 4°C. Finally, the slides were washed with PBST solution and incubated with Alexa Fluor 555-conjugated goat anti-rabbit IgG secondary antibody at the dilution of 1:2,000 for 1 h at RT, followed by application of DAPI (10 μg/mL in PBS) for 10 min to stain the nuclei. Fluorescence imaging was collected by confocal fluorescence microscopy (Leica).

Western Blot Analysis

MCF-7 cells (1×10^5/dish) were plated in 10-cm dishes and treated with 100 nM BPA or BPS for 48 h. Cells were collected by resuspension in the cell lysis buffer for Western blot and IP (Beyotime), incubated on ice for 30 min, and centrifuged at $12{,}000 \times g$ for 10 min at 4°C. The supernatant was collected, and the protein content was quantified using a bicinchoninic acid (BCA) protein assay kit (Beyotime). Protein samples (50 μg) were separated on a 10% sodium dodecyl sulfate (SDS)-polyacrylamide gel and transferred to a polyvinylidene difluoride membrane (Millipore). After washing with PBST three times, the membranes were blocked with 5% nonfat milk for 30 min and then incubated with primary antibodies overnight at 4°C. The blots were then washed with PBST three times and incubated with appropriate (anti-rabbit or anti-mouse) secondary antibodies conjugated to IRDye680 or IRDye800 fluorescence dye. After washing with PBST three times, the protein bands were detected using an Odyssey Infrared Imaging system (Li-COR Biosciences). The primary antibodies for TET1, TET2, TET3, DNA methyltransferase (DNMT)1, DNMT3A, DNMT3B, ERα, ERβ, and SP1 were used at the dilution of 1:1,000, and the secondary antibodies were used at the dilution of 1:2,000 (see Table S1). The relative intensity was analyzed with ImageJ software (version 1.47) (Schneider et al. 2012) and calculated by the ratio relative to the glyceraldehyde 3-phosphate dehydrogenase (GAPDH) intensity. For the evaluation of different blots, each band of the replicates was normalized to GAPDH and then averaged. The averaged intensities were taken for comparison.

Total RNA Extraction and Quantitative Reverse Transcription–Polymerase Chain Reaction

Total RNA was extracted from the harvested MCF-7 cells according to the manufacturer's instructions using TRI reagent (Sigma). The concentration of RNA was determined by measuring OD at 260 nm. First-strand complementary DNA (cDNA) was synthesized with the SuperScript II First-Strand Synthesis System for quantitative reverse transcription–polymerase chain reaction (qRT-PCR; Invitrogen). qPCR amplification was carried out using actin as an endogenous control. SYBR Green probes for each gene were used. The primers are listed in Table S2. Real-time PCR was carried out using 50 ng of cDNA and SYBR PCR master mix (TaKaRa) in the Agilent Mx3000P Real-time PCR System with the two-step procedure (95°C 2 min, 1 cycle; 95°C 15 s, 60°C 1 min, 30 cycles). Relative quantitation of each single gene expression was performed using the comparative threshold cycle method.

Total TET Activity Determination by ELISA

Total TET activity was analyzed using a fluorescence-based ELISA kit according to the instructions provided by the manufacturer (Epigentek). This assay involves the conversion of 5mC substrate, coated onto microplate wells, by the TET enzymes in the sample, resulting in the conversion of 5mC to 5hmC, which in turn is detected fluorometrically using a specific antibody. MCF-7 cells (1×10^5/dish) were seeded in 6-cm dishes for 24 h and then treated with BPA or BPS (10–1,000 nM) for 48 h for the subsequent nuclear extracts. Nuclear extracts were prepared using a nuclear extract

preparation kit (Active Motif), and the protein concentrations were determined using a BCA protein assay kit (Beyotime Biotechnology). Then 5 μg of the nuclear extract was used for the TET activity assay, and the relative fluorescence intensity was measured at excitation 530 nm and emission 590 nm using a microplate reader (Varioskan Flash, Thermo). Data were expressed as relative fluorescence units.

Short Hairpin RNA Knockdown

The short hairpin RNAs (shRNAs) were designed and chemically synthesized by Sangon. The shRNAs were annealed in a thermocycler at 95°C for 5 min with a cooldown at RT for 1 h and cloned into a short interfering RNA-expressing vector named pSilencer4.1 (purchased from Addgene) using the restriction–ligation method with BamHI (Catalog No. R3136, NEB) and T4 DNA ligase (Catalog No. M0202, NEB). The shRNA-targeted sequences are listed in Table S3. Purified plasmids were transfected into MCF-7 cells at 40–60% confluency with Lipofectamine 2000 (Invitrogen Life Technologies) according to the manufacturer's instructions. After culture for 2 d, the transfected cells were selected using the geneticin G418 (500 μg/mL) for 5 d.

CRISPR/cas9 Knockout

For CRISPR/cas9 knockout, the guide RNAs (gRNAs) for ERα (forward: 5′-CACCGCGCCTACGAGTTCAACGCCG-3′; reverse: 5′-AAACCGGCGTTGAACTCGTAGGCGC-3′) and ERβ (forward: 5′-CACCGCCGTGTACAACTACCCCGA-3′; reverse: 5′-AAACTCGGGGTAGTTGTACACGGC-3′) were designed and chemically synthesized by Sangon. The gRNAs were then annealed by heating at 95°C for 5 min with a cooldown at RT for 1 h and cloned into a PX458 vector with a green fluorescent protein (GFP) label (purchased from Addgene) by the restriction–ligation method with estriction endonuclease BbsI (Catalog No. R3539, NEB) and T4 DNA ligase (Catalog No. M0202, NEB). MCF-7 cells (purchased from ATCC) at a density of 1×10^4 cells/well on 24-well plates were transfected with 5 μg of PX458. After culture in 5% CO_2 at 37°C for 24 h, cells were selected by GFP fluorescence using BD AriaII flow cytometry, then cultured for 7 d for isolating single-cell clones.

Construction of pcDNA3-FLAG-TET2 and Cell Transfection

The pcDNA3-FLAG-TET2 was constructed by insertion of the open reading frame of TET2 into the pcDNA3-FLAG vector (purchased from Addgene) by homologous recombination using High-Fidelity *Taq* DNA Ligase (NEB). The primers for the cloning of the open reading frame of TET2 were as follows: (forward: 5′-TATAGGGAGACCCAAGCTTGGTACATGGAACAGGATAGAACCAACC-3′; reverse: 5′-TCGTCCTTGTAGTCCATGTCGGTACTCATATATA-TCTGTTGTAAGGC-3′). The constructed plasmid was amplified in *Escherichia coli* (Catalog No. 9057, TaKaRa), cultured in a shaker at 37°C for 12 h. Plasmids were then extracted using the EndoFree Maxi Plasmid Kit (Catalog No. DP117, TIANGEN) and verified by Sanger sequencing (Sangon). MCF-7 cells (1×10^4 cells/well) seeded on 24-well plates were transfected with 5 μg of the verified plasmid using Lipofectamine 2000 (Invitrogen Life Technologies) according to the manufacturer's protocol. MCF-7 cells were serum-starved overnight 24 h after transfection and then cultured in 5% CO_2 at 37°C.

Co-Immunoprecipitation

The MCF-7 cells (1×10^5/dish) were cultured on 6-cm dishes and treated with 100 nM BPA, 100 nM BPS, or vehicle for 48 h. At the end of treatment, the MCF-7 cells were rinsed three times with ice-cold PBS buffer, followed by incubation for 30 min at 4°C with 1 mL ice-cold IP lysis buffer (Beyotime) containing the serine protease inhibitor phenylmethanesulfonyl fluoride (PMSF). Cell lysates were then centrifuged at $12{,}000 \times g$ for 20 min at 4°C. Supernatants were collected and the protein concentrations were determined by a BCA protein assay kit (Beyotime Biotechnology). Cell extracts were incubated with anti-ERα or anti-IgG antibody (at the dilution of 1:1,000) plus protein G–conjugated Sepharose beads (Amersham Pharmacia) in a ratio of 1 μg of extract per 30 μL of beads. After overnight rocking at 4°C, the precipitates were collected by centrifugation at $2{,}500 \times g$ for 3 min and washed with ice-cold IP lysis buffer (Beyotime) three times, then subjected to SDS-polyacrylamide gel electrophoresis and Western blotting with anti-ERα, anti-TET2, and anti-SP1 antibodies.

Bisulfite Sequencing-PCR of TET2 CpG Islands

MCF-7 cells (1×10^5/dish) were plated in 6-cm dishes for 24 h, followed by treatments with 100 nM BPA, 100 nM BPS, or vehicle for 48 h, and the genomic DNA was then extracted from the harvested MCF-7 cells using a Genomic DNA Purification Kit (Promega). The specific primers for TET2 promoter region (forward: 5′-TTTTTTTTTAGGGGTGGA-3′; reverse: 5′-ACTTACATACGAACGAAACCC-3′) was designed by Methyl Primer Express™ (version 1.0; ThermoFisher). Bisulfite treatments of the genomic DNA samples were carried out with the Qiagen EpiTect kit according to the manufacturer's instructions, followed by the PCR amplification procedure (98°C 30 s; 98°C 10 s, 60°C 30 s, 72°C 10 s, 35 cycles; 72°C 2 min; 4°C hold) using Q5 Hot Start High-Fidelity Master Mix (NEB). The PCR products were identified by electrophoresis and gel-purified with the Gel and PCR Clean-up System (Promega). The purified PCR products were inserted into pCR™4Blunt-TOPO® Vector using the Zero Blunt™ TOPO™ PCR Cloning Kit (Invitrogen) and sequenced by Sanger sequencing (Sangon).

Chromatin Immunoprecipitation-qPCR

Chromatin immunoprecipitation-qPCR (ChIP) assays were performed for MCF-7 cells using the SimpleChIP Plus Enzymatic Chromatin IP Kit (Cell Signaling Technology) according to the manufacturer's instructions. MCF-7 cells (1×10^5/dish) were plated in 6-cm dishes for 24 h and treated with 100 nM BPA, 100 nM BPS, or vehicle for 48 h. Precipitated DNA from the MCF-7 cells was dissolved in 50 μL of Tris-EDTA (TE) buffer and subjected to qPCR using the Agilent Mx3000P Real-time PCR System. The primers for ChIP-qPCR assay are listed in Table S4.

Statistical Analysis

All assays were repeated independently a minimum of three times ($n \geq 3$), and three wells per assay were used for each treatment in each cell line. We averaged the data to arrive at a single (mean) value per treatment per cell line per time per replicate. The experimental data were expressed as the mean ± standard deviation (SD), and the raw data used to generate all bar graphs are listed in the supplemental Excel files. Differences among treatments were evaluated by two-way analysis of variance (with Bonferroni posttest), and the statistical comparisons of two treatments were determined by Student's paired *t*-tests using SPSS® statistical software (version 22.0; IBM). The statistical significance was indicated by * for $p < 0.05$, ** for $p < 0.01$, and $^{\#}$ for $p < 0.05$.

Results

Proliferation of BPA/BPS-Treated Breast Cancer Cells

First, we examined the effects of BPA/BPS on the proliferation of breast cancer cells (MCF-7, T47D, and MDA-MB-231 cells). Both BPA and BPS treatments (10–1,000 nM) promoted the proliferation of ER^+ MCF-7 over 24–72 h (Figure 1A,B), except that of 72 h × 100 nM and 72 h × 1,000 nM BPA/BPS treatment. Using endogenous E_2 as the positive control, the proliferation effects of 100 nM BPA/BPS were equivalent to that of 1 nM E_2 (see Figure S1A). BPA/BPS treatment also consistently promoted the proliferation of T47D cells, but the proliferation efficiency

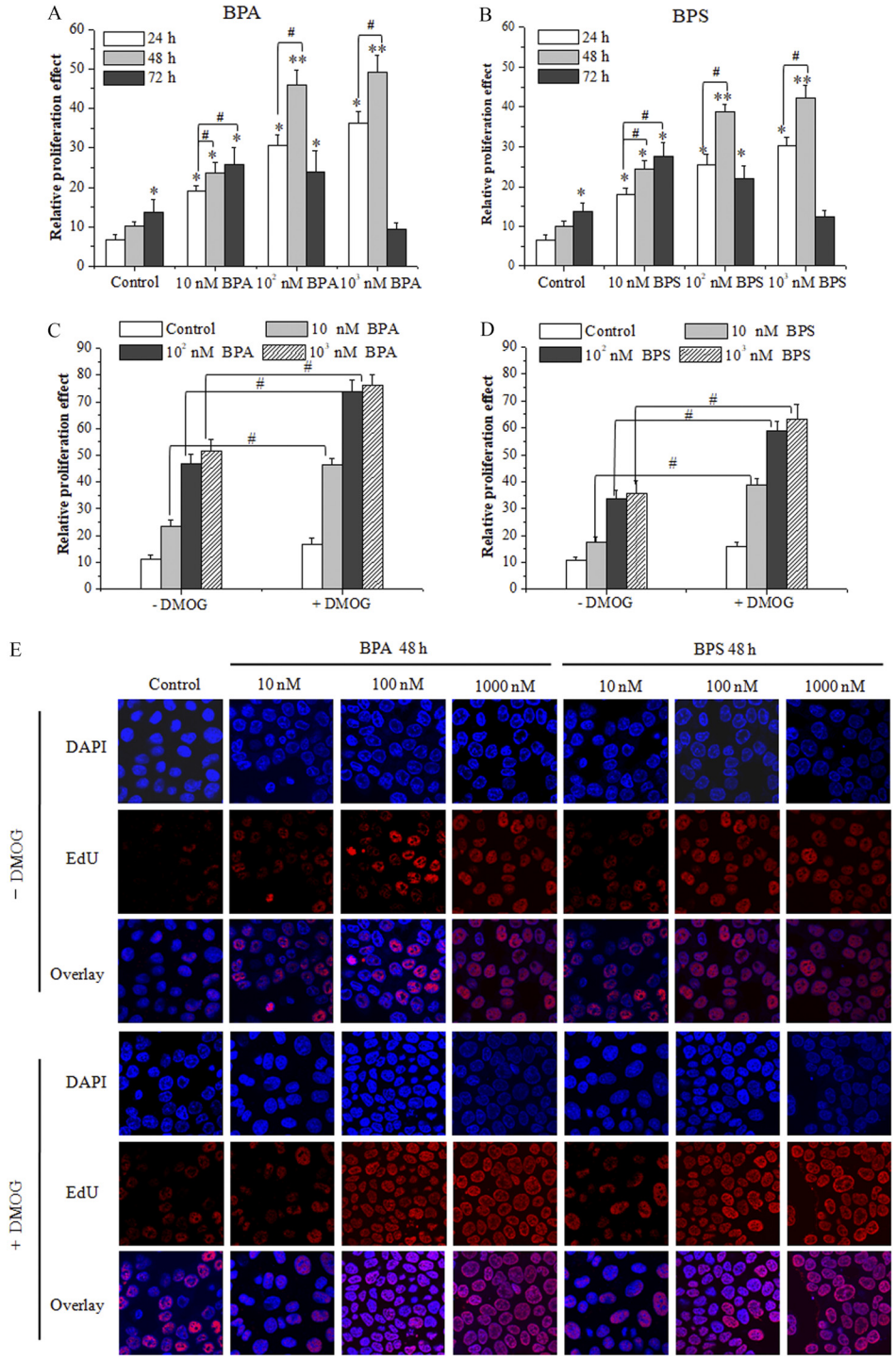

Figure 1. Proliferation of bisphenol A (BPA)- or bisphenol S (BPS)-treated MCF-7 breast cancer cells. (A,B) MTS assay of MCF-7 cell proliferation induced by BPA/BPS. The data of mean ± SD (five replicates) are shown. Statistical analysis was performed with two-way ANOVA (with Bonferroni posttest). (C,D) MTS assay of the effect of dimethyloxaloylglycine (DMOG) on BPA/BPS-stimulated MCF-7 proliferation. Data represent mean ± SD of five independent experiments. Statistical analysis was performed with Student's paired *t*-test. (E) 5-Ethynyl-2′-deoxyuridine (EdU) assay of the effect of DMOG on BPA/BPS-stimulated MCF-7 proliferation. MCF-7 cells were pretreated with DMOG for 24 h and then subjected to BPA or BPS exposure for 48 h. *, $p < 0.05$ or **, $p < 0.01$ vs. control of 24 h; $^{\#}$, $p < 0.05$ vs. indicated samples. Note: ANOVA, analysis of variance; DAPI, 4′,6-diamidino-2-phenylindole; MTS, a tetrazolium salt; SD, standard deviation.

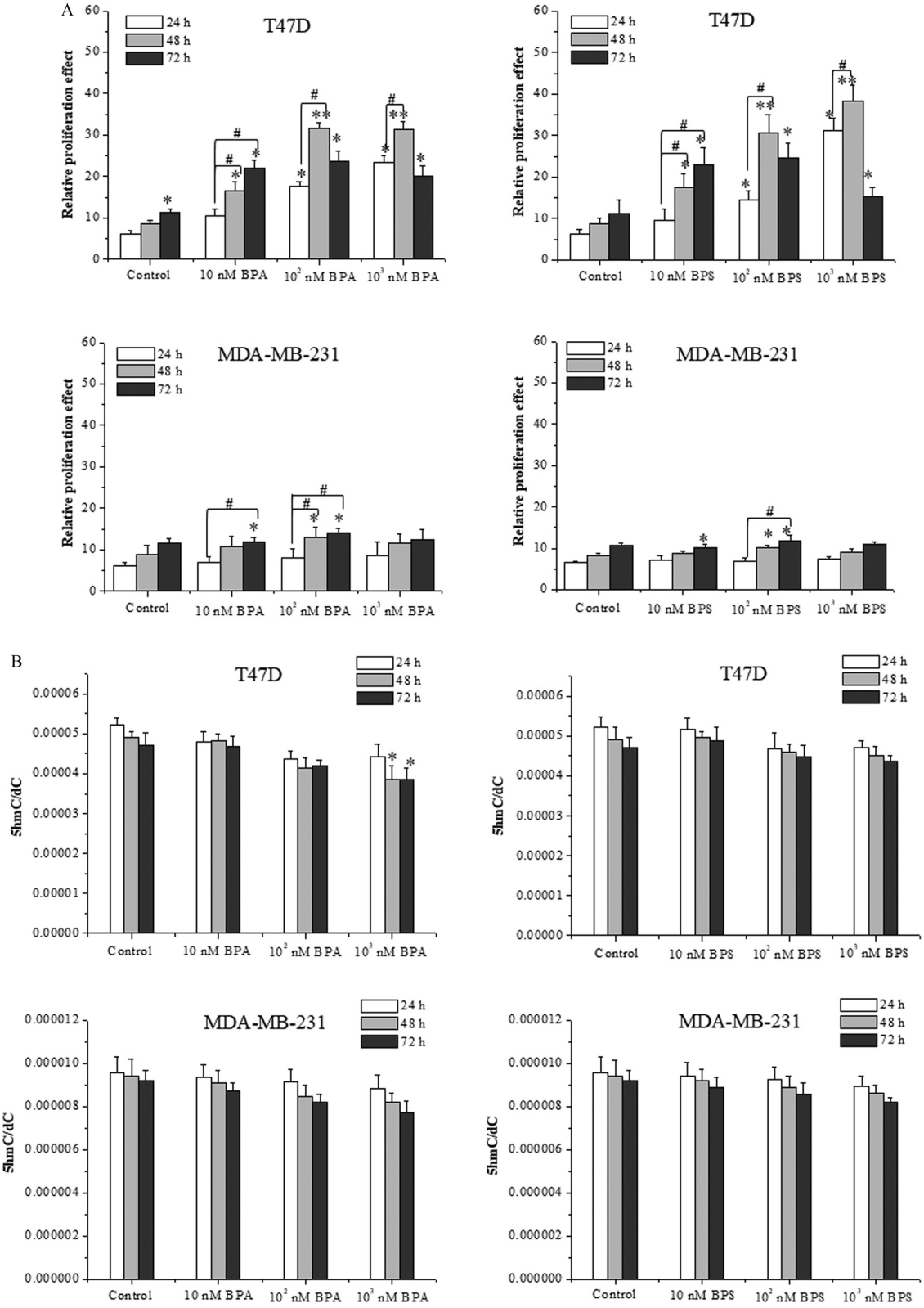

Figure 2. Proliferation and genomic 5-hydroxymethylcytosine (5hmC) level of T47D and MDA-MB-231 breast cancer cells treated with bisphenol A (BPA) or bisphenol S (BPS). (A) MTS assay of BPA/BPS-treated T47D and MDA-MB-231 cells. (B) Detection of genomic DNA 5hmC level by UHPLC-MRM MS/MS analysis in T47D and MDA-MB-231 cells upon BPA or BPS treatment. For each combination of treatment and time point, the mean and corresponding ± SD (of three replicates) are shown. Statistical analysis was performed with two-way ANOVA (with Bonferroni posttest). *, $p < 0.05$ or **, $p < 0.01$ vs. control of 24 h; $^{\#}$, $p < 0.05$ vs. indicated samples. Note: ANOVA, analysis of variance; MTS, a tetrazolium salt; SD, standard deviation; UHPLC-MRM MS/MS, ultra-high performance liquid chromatography–tandem mass spectrometry.

was lower than that of MCF-7 cells (Figure 2A). BPA/BPS exposure had no notable effect on the proliferation of triple-negative MDA-MB-231 cells (Figure 2A).

Based on above results, we felt that MCF-7 was an excellent ER^+ cell line, representing a strong proliferation response to BPA/BPS. Hence, we extensively used the MCF-7 cells for the following experiments.

We further examined the possibility of TET dioxygenases involved in BPA/BPS-promoted proliferation. Surprisingly, DMOG (200 mM, 48 h), a cell-permeable competitor of TET cofactor α-ketoglutarate (α-KG), could further stimulate the proliferation of MCF-7 cells upon BPA/BPS exposure (Figure 1C,D). To further validate these observations, we used the EdU probe to detect cell proliferation (Figure 1E). Consistently, as shown by fluorescence imaging, both BPA and BPS treatments (10–1,000 nM, 48 h) promoted the proliferation of MCF-7 cells. Although DMOG treatment slightly increased the proliferation of control cells, BPA and BPS treatments (10–1,000 nM, 48 h) induced greater proliferation in DMOG-treated MCF-7 cells than in cells not treated with DMOG (Figure 1E).

Genomic DNA Hydroxymethylation in BPA/BPS-Treated Breast Cancer Cells

To verify whether TET dioxygenases are involved in BPA/BPS-promoted cell proliferation, we examined genomic 5hmC in MCF-

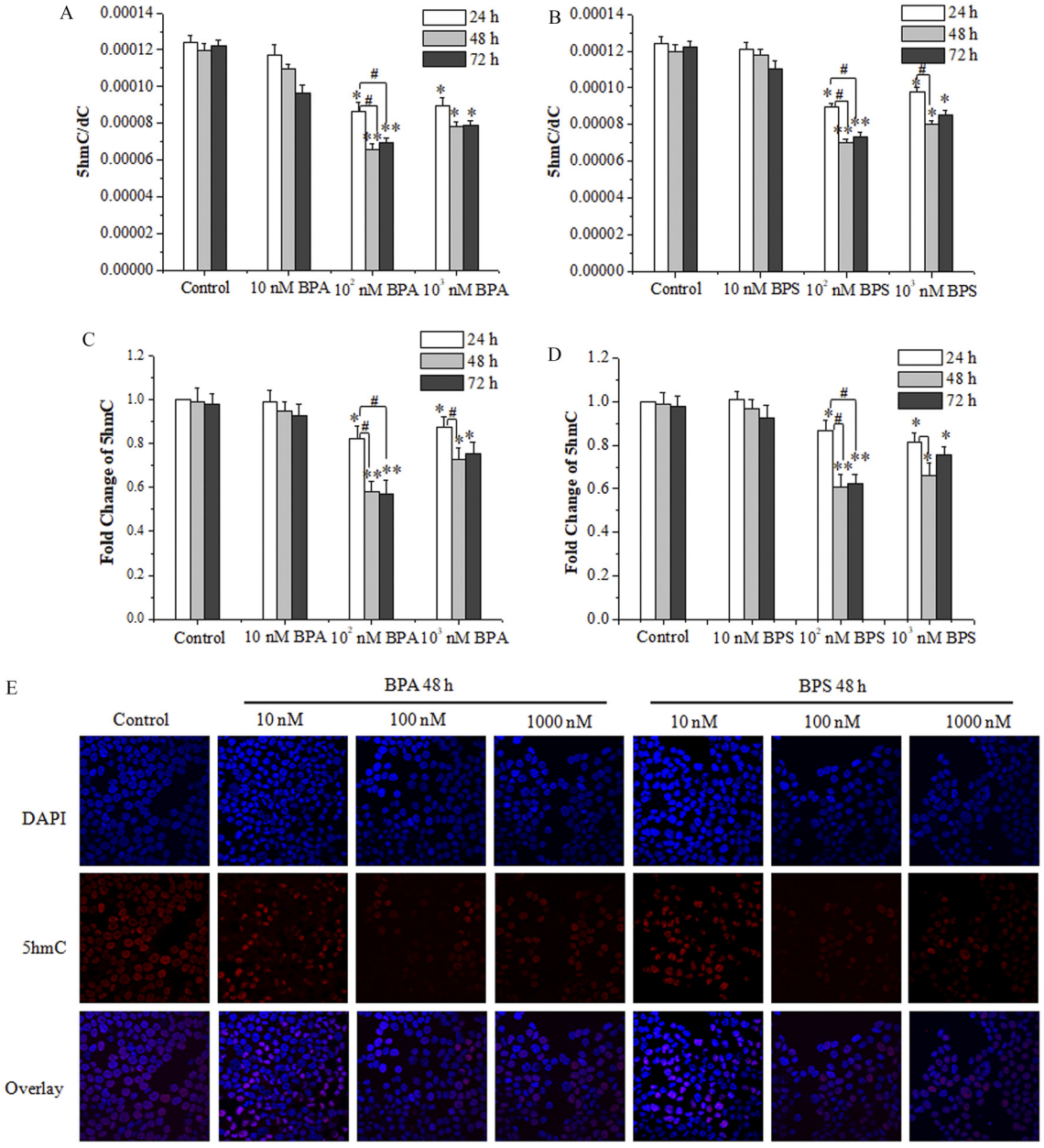

Figure 3. Genomic DNA 5-hydroxymethylcytosine (5hmC) level in bisphenol A (BPA)- or bisphenol S (BPS)-treated MCF-7 cells. (A,B) 5hmC frequency measured by UHPLC-MRM MS/MS analysis of enzymatically digested genomic DNA from MCF-7 cells exposed to BPA (A) and BPS (B). (C,D) Relative level of genomic 5hmC measured by ELISA of genomic DNA from MCF-7 cells exposed to BPA (C) and BPS (D). (E) Immunofluorescence analysis of 5hmC in MCF-7 cells exposed to BPA and BPS. The data of mean ± SD (five replicates) are shown. Statistical significance was evaluated by two-way ANOVA (with Bonferroni posttest). *, $p < 0.05$ or **, $p < 0.01$ vs. control of 24 h; $^{\#}$, $p < 0.05$ vs. indicated samples. Note: ANOVA, analysis of variance; DAPI, 4′,6-diamidino-2-phenylindole; ELISA, enzyme-linked immunosorbent assay; SD, standard deviation; UHPLC-MRM MS/MS, ultra-high performance liquid chromatography–tandem mass spectrometry.

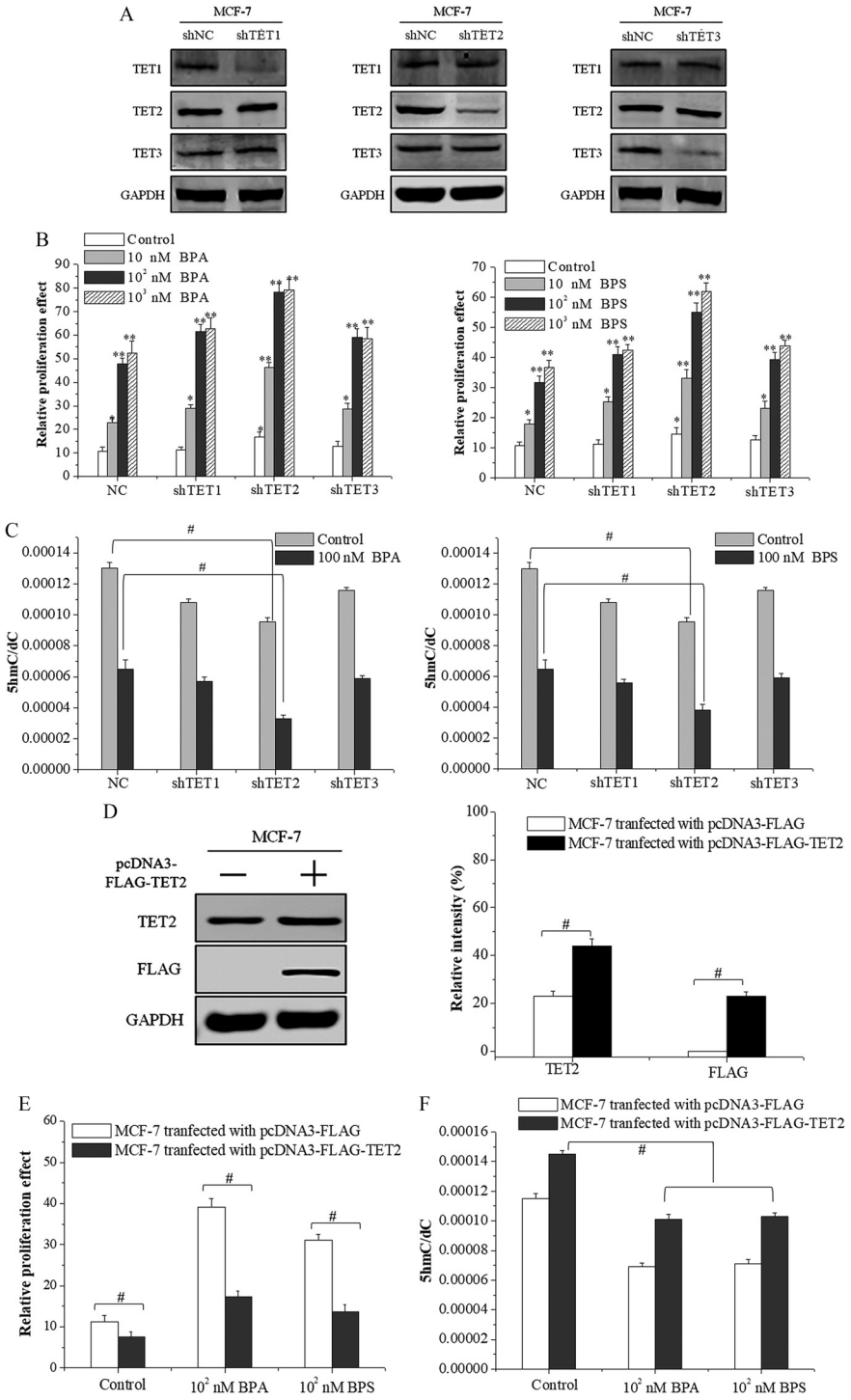

Figure 4. Cell proliferation and 5-hydroxymethylcytosine (5hmC) level in ten-eleven translocation 2 (TET2)-knockdown and TET2-overexpression MCF-7 cells treated with bisphenol A (BPA) or bisphenol S (BPS). (A) Identification of the short hairpin RNA (shRNA)-transfected MCF-7 cell lines using Western blot. (B) Cell proliferation assay by MTS of shRNA-transfected MCF-7 cells exposed to vehicle, BPA, or BPS. Data represent mean ± SD of five independent experiments. Statistical analysis was evaluated by two-way ANOVA (with Bonferroni posttest). *, $p < 0.05$ or **, $p < 0.01$ vs. control of cells transfected with shNC (NC). (C) UHPLC-MRM MS/MS analysis of 5hmC in the enzymatic digest of genomic DNA from shRNA-transfected MCF-7 cells exposed to vehicle, BPA, or BPS. Data represent mean ± SD of five independent experiments. Statistical analysis was performed with two-way ANOVA (with Bonferroni posttest). $^{\#}$, $p < 0.05$ vs. indicated samples. (D) Identification of TET2 protein in MCF-7 cells transfected with pcDNA3-FLAG-TET2 plasmid using Western blot. The relative intensity was analyzed with ImageJ software (Schneider et al. 2012) and calculated by the ratio relative to the GAPDH intensity. Data represent mean ± SD of three independent experiments. Statistical analysis was performed with Student's paired *t*-test. $^{\#}$, $p < 0.05$ vs. indicated samples. (E) Cell proliferation assay by MTS of MCF-7 cells transfected with pcDNA3-FLAG-TET2 exposed to vehicle, BPA, or BPS. Data represent mean ± SD of five independent experiments. Statistical analysis was performed with Student's paired *t*-test. $^{\#}$, $p < 0.05$ vs. indicated samples. (F) 5hmC frequency measured by UHPLC-MRM MS/MS analysis of digested genomic DNA from MCF-7 cells transfected with pcDNA3-FLAG-TET2 exposed to vehicle, BPA, or BPS. Data represent mean ± SD of five independent experiments. Statistical analysis was performed with Student's paired *t*-test. $^{\#}$, $p < 0.05$ vs. indicated samples. Note: ANOVA, analysis of variance; GAPDH, glyceraldehyde 3-phosphate dehydrogenase; MTS, a tetrazolium salt; SD, standard deviation; UHPLC-MRM MS/MS, ultra-high performance liquid chromatography–tandem mass spectrometry.

7 cells (Figure 3). Ultrasensitive UHPLC-MS/MS analysis showed that BPA/BPS treatment (10–1,000 nM, 24–72 h), induced a significant decrease in the level of genomic 5hmC. The dosing regimen in which the greatest difference in 5hmC (40%) between treated and control was seen under the 48 h × 100 nM BPA/BPS treatment compared with the control group (Figure 3A,B), which was almost equivalent to that of 1 nM E_2 (see Figure S1B). Similar results were obtained from the quantification assay of 5hmC level using an ELISA kit (Figure 3C,D), and the immunofluorescence assay also confirmed that the genomic 5hmC was visibly lower after BPA/BPS treatment (Figure 3E).

BPA/BPS treatment could also result in lower in genomic 5hmC content in the T47D cells, but much less than that in MCF-7 cells (Figure 2B). In contrast, BPA/BPS had no significant effect on the 5hmC level in triple-negative MDA-MB-231 cells (Figure 2B).

TET2 Expression in BPA/BPS-Treated Breast Cancer Cells

As the enzymes catalyzing 5hmC formation, the expression of TET dioxygenases (TET1, TET2, and TET3) were examined after BPA/BPS exposure in MCF-7 cells. qRT-PCR analysis showed that the transcription level of TET2 in MCF-7 cells was

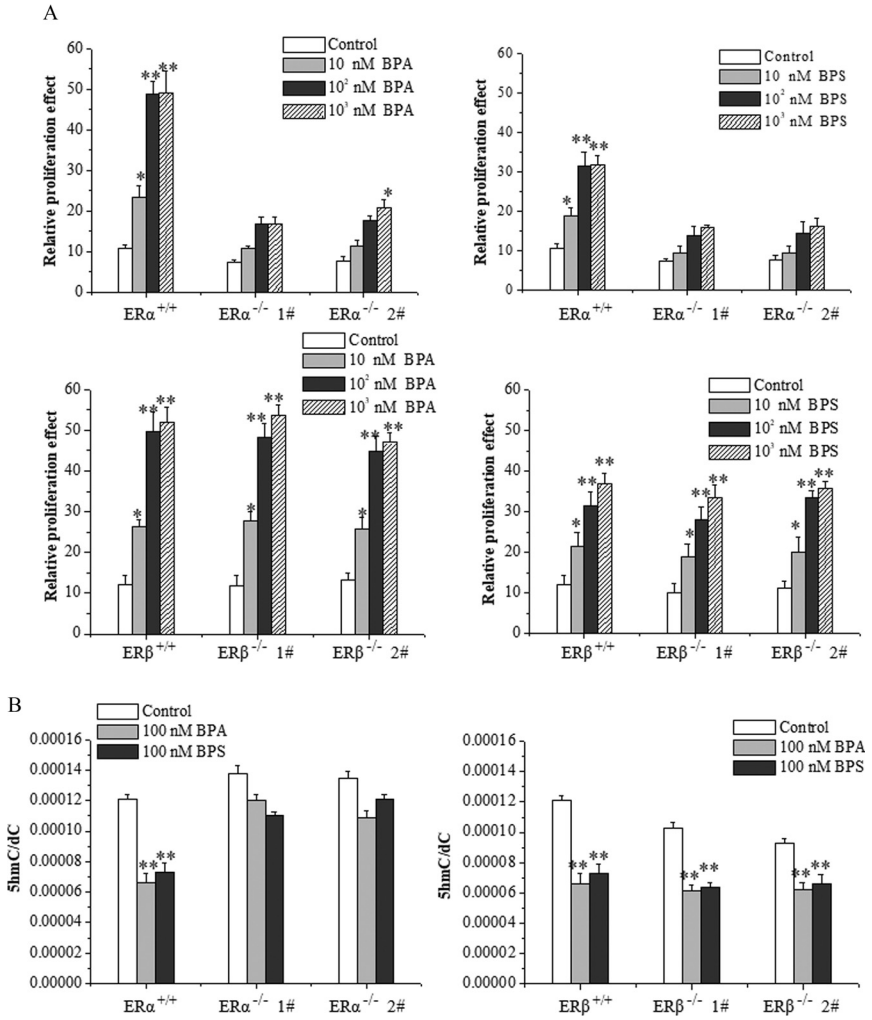

Figure 5. Cell proliferation, 5-hydroxymethylcytosine (5hmC) level, and ten-eleven translocation 2 (TET2) expression in estrogen-receptor-knockout MCF-7 cells treated with bisphenol A (BPA) or bisphenol S (BPS). (A) Cell proliferation assay by MTS of $ER\alpha^{-/-}$ and $ER\beta^{-/-}$ MCF-7 cells exposed to vehicle, BPA, or BPS. Data represent mean ± SD of five independent experiments. Statistical analysis was performed with two-way ANOVA (with Bonferroni posttest): *, $p < 0.05$ or **, $p < 0.01$ vs. control of $ER\alpha^{+/+}$ or $ER\beta^{+/+}$ cells. (B) 5hmC frequency measured by UHPLC-MRM MS/MS analysis of digested genomic DNA from $ER\alpha^{-/-}$ and $ER\beta^{-/-}$ MCF-7 cells exposed to vehicle, BPA, or BPS. Data represent mean ± SD of five independent experiments. Statistical analysis was performed with two-way ANOVA (with Bonferroni posttest). *, $p < 0.05$ or **, $p < 0.01$ vs. control of $ER\alpha^{+/+}$ or $ER\beta^{+/+}$ cells. (C) Quantification of Western blot detection of TET1, TET2, and TET3 proteins in $ER\alpha^{-/-}$ MCF-7 cells at 48 h after vehicle, BPA, or BPS treatment. The relative intensity was analyzed with ImageJ software (Schneider et al. 2012) and calculated by the ratio relative to the GAPDH intensity. Data represent mean ± SD of three independent experiments. Statistical analysis was performed with Student's paired *t*-test. *, $p < 0.05$ vs. control. (D) Identification of TET2 protein in $ER\alpha^{-/-}$ MCF-7 cells transfected with short hairpin RNA (shRNA)-TET2 plasmid using Western blot. The relative intensity was analyzed with ImageJ software and calculated by the ratio relative to the GAPDH intensity. Data represent mean ± SD of three independent experiments. Statistical analysis was performed with Student's paired *t*-test. $^{\#}$, $p < 0.05$ vs. indicated samples. (E) Cell proliferation assay by MTS of $ER\alpha^{-/-}$ MCF-7 cells transfected with shRNA-TET2 exposed to BPA and BPS. Data represent mean ± SD of five independent experiments. Statistical analysis was performed with two-way ANOVA (with Bonferroni posttest). *, $p < 0.05$ or **, $p < 0.01$ vs. $ER\alpha^{+/+}$ of each treatment. (F) 5hmC frequency measured by UHPLC-MRM MS/MS analysis of digested genomic DNA from $ER\alpha^{-/-}$ MCF-7 cells transfected with shRNA-TET2 exposed to BPA and BPS. Data represent mean ± SD of five independent experiments. Statistical significance was evaluated by two-way ANOVA (with Bonferroni posttest). *, $p < 0.05$ or **, $p < 0.01$ vs. control of $ER\alpha^{+/+}$ cells. Note: ANOVA, analysis of variance; GAPDH, glyceraldehyde 3-phosphate dehydrogenase; MTS, a tetrazolium salt; SD, standard deviation; UHPLC-MRM MS/MS, ultra-high performance liquid chromatography–tandem mass spectrometry.

significantly higher than that of TET1 and TET3, whereas the expression of TET2 in MCF-7 cells was notably lower after 48 h × 100 nM BPA/BPS treatment (see Figure S2A). Immunoblotting assay showed that the protein level of TET2 was highest among the three TET dioxygenases in untreated MCF-7 cells, and 100 nM BPA/BPS treatment reduced the expression of TET2 protein (see Figure S2B,C). As a positive control, 1.0 nM E_2 treatment induced the inhibitory effects on the TET2 expression similar to the exposure of 100 nM BPA/BPS (see Figure S1C–E).

Effects of TET2 on the BPA/BPS-Stimulated Proliferation of Breast Cancer Cells

To further investigate the role of TET dioxygenases in BPA/BPS-induced proliferation of MCF-7 cells, we designed shRNA expression vectors for TET1, TET2, and TET3 to construct the knockdown cells of MCF-7, respectively. Western blotting analysis showed that the transfection of TET1-shRNA, TET2-shRNA, and TET3-shRNA plasmids reduced only the target protein effectively, whereas the expression of the other two proteins was not affected (Figure 4A). MCF-7 cells transfected with TET2-shRNA displayed higher proliferation when treated with BPA/BPS (48 h × 100 nM) than those transfected with TET1- or TET3-shRNA (Figure 4B). Meanwhile, the genomic 5hmC level and TET2 protein expression in MCF-7 cells transfected with TET2-shRNA decreased significantly compared with the control group (Figure 4C; see also Figure S3A,B). There was a trend that the genomic 5hmC levels in MCF-7 cells transfected with TET1- or TET3-shRNA were lower (compared with the control cells), but it did not reach statistical significance to be accurate (Figure 4C). For further confirmation, the second shRNA constructs for each TET gene were used and similar results were obtained (see Figure S4).

To verify the role of TET2 in the proliferation of MCF-7 cells, we constructed a pcDNA3-FLAG-TET2 plasmid that was transfected into MCF-7 cells to obtain the TET2 overexpression cell lines. Western blot analysis showed that the transfection of the pcDNA3-FLAG-TET2 plasmid in MCF-7 cells increased the expression of TET2 by 91.3 ± 3.5% compared with that of control group (Figure 4D). Meanwhile, MTS assay showed that the TET2 overexpression reduced the BPA/BPS-stimulated proliferation of MCF-7 cells (Figure 4E) and that the genomic 5hmC content and TET2 protein expression increased significantly compared with that of the control group (Figure 4F; see also Figure S3C,D). Of note, DMOG, an inhibitor repressing the catalytic oxidation activity of TET dioxygenases on DNA 5mC, promoted the proliferation of MCF-7 cells (Figure 1D).

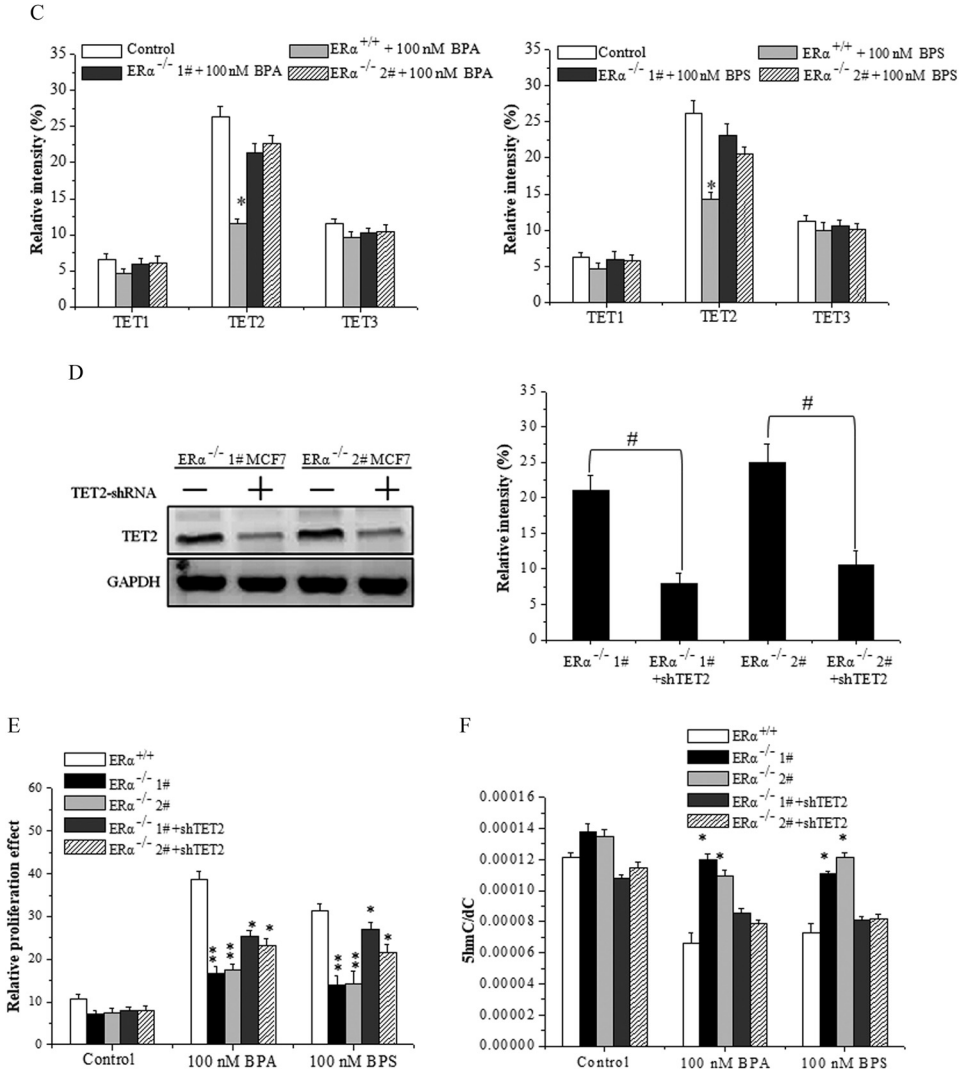

Figure 5. (*Continued.*)

Influences of ERα Activation on the TET2 Expression and DNA Hydroxymethylation in BPA/BPS-Treated Breast Cancer Cells

We next examined the total ER protein expression and phosphorylation at different ERα and ERβ sites in MCF-7 cells exposed to BPA and BPS. Western blotting analysis showed that BPA/BPS treatment did not significantly change the total protein expression of ERα but, rather, increased its phosphorylation levels at the S118, S167, S305, and T311 sites, especially at the S118 and S167 sites (see Figure S5A,C). At the same time, Western blot analysis showed that the total protein expression of ERβ and its phosphorylation levels at sites S87 and S105 of ERβ did not change significantly upon BPA/BPS exposure (see Figure S5B,D).

In order to further elucidate the roles of activated ERs in the BPA/BPS-stimulated proliferation of MCF-7 cells, we constructed ERα$^{-/-}$ and ERβ$^{-/-}$ MCF-7 cells using the Crispr/Cas9 technique. The knockout effect was verified by sequencing (see Figure S6A) and Western blot (see Figure S6B). The MTS assay consistently showed that the depletion of ERα, but not ERβ, repressed the proliferation of MCF-7 cells upon BPA/BPS exposure (Figure 5A). UHPLC-MS/MS analysis revealed that the genomic 5hmC content of ERα$^{-/-}$ MCF-7 cells was significantly higher than that in wild-type cells (Figure 5B), whereas that of ERβ$^{-/-}$ MCF-7 exhibited no obvious difference (Figure 5B).

Next, we focused on the effects of BPA/BPS on expression of TETs in ERα$^{-/-}$ cells. Upon BPA/BPS exposure, both the transcriptional mRNA and protein of TET2 maintained a higher level in the ERα$^{-/-}$ MCF-7 cells than that of ERα$^{+/+}$ MCF-7 cells (Figure 5C; see also Figures S7A and S8). In contrast, whether ERβ was depleted or not, BPA/BPS exposure consistently reduced the expression of TET2 (see Figure S7B). Furthermore, we observed that the TET2 knockdown alleviated the ERα knockout-caused inhibition in proliferation but reduced the genomic 5hmC content upon BPA/BPS exposure in ERα$^{-/-}$ MCF-7 cells (Figure 5D–F).

Impacts of BPA/BPS-Stimulated ERα on the Promoter Methylation of the TET2 Gene

The above results motivated us to find out how ERα affects TET2 in ER^{+} breast cells upon BPA/BPS exposure. To do this, we examined the interaction of ERα and TET2 protein and gene silence-associated promoter methylation of TET2. As revealed by Co-IP analysis, we did not observe any direct interaction between ERα and TET2 protein (see Figure S9). Using BSP to target a 423-bp CpG island (containing 54 paired CpGs) (Figure 6A), we observed that the methylation ratio dramatically increased from about $32.1 \pm 3.2\%$ for the control MCF-7 (Figure 6B,C) up to $77.5 \pm 5.1\%$ and $68.3 \pm 4.6\%$ for the MCF-7 cells with the respective BPA and BPS treatments (48 h × 100 nM). On the contrary, ERα depletion reduced the methylation ratio of MCF-7 cells ($19.3 \pm 2.9\%$), and exposure to BPA or BPS caused a moderate increase in the methylation ratio (30.1–39.2%), which was much lower than that of ERα$^{+/+}$ MCF-7 cells (Figure 6B,C).

Roles of ERα-Regulated DNMTs Expression in the Promoter Methylation of the TET2 Gene under BPA/BPS Exposure

The promoter methylation is catalyzed by DNA methyltransferases (DNMTs). We observed that the transcriptional and protein levels of DNMT1, DNMT3A, and DNMT3B significantly increased

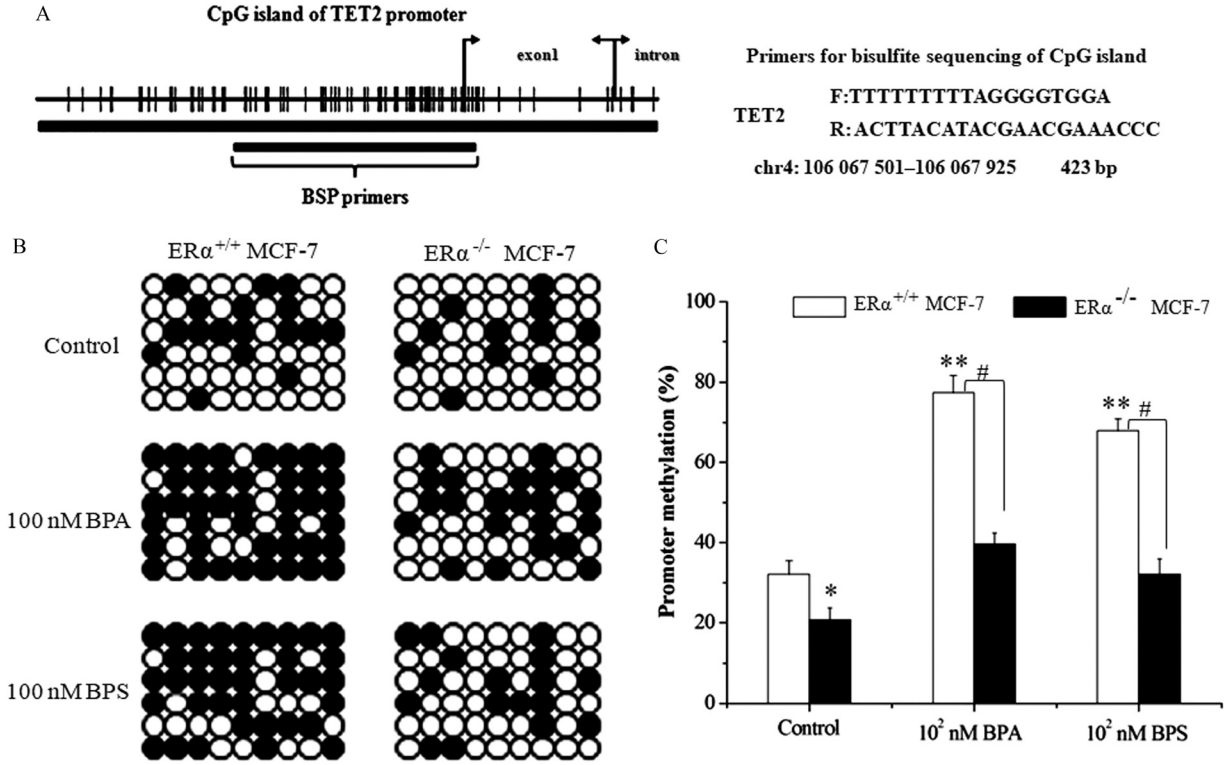

Figure 6. Detection of interaction between ERα and ten-eleven translocation 2 (TET2) under bisphenol A (BPA) or bisphenol S (BPS) exposure using bisulfite sequencing-PCR (BSP). (A) CpG island of TET2 gene with location and sequence of methylation-specific primers. (B,C) DNA sequencing analysis (B) and quantitative statistics (C) of methylation-specific PCR product of TET2 promoter in ERα$^{+/+}$ and ERα$^{-/-}$ MCF-7 cells exposed to vehicle, BPA, or BPS. Data represent mean ± SD of five independent experiments. Statistical significance was evaluated by two-way ANOVA (with Bonferroni posttest). *, $p < 0.05$ or **, $p < 0.01$ vs. control of ERα$^{+/+}$ cells; $^{\#}$, $p < 0.05$ vs. indicated samples. Note: ANOVA, analysis of variance; PCR, polymerase chain reaction; SD, standard deviation.

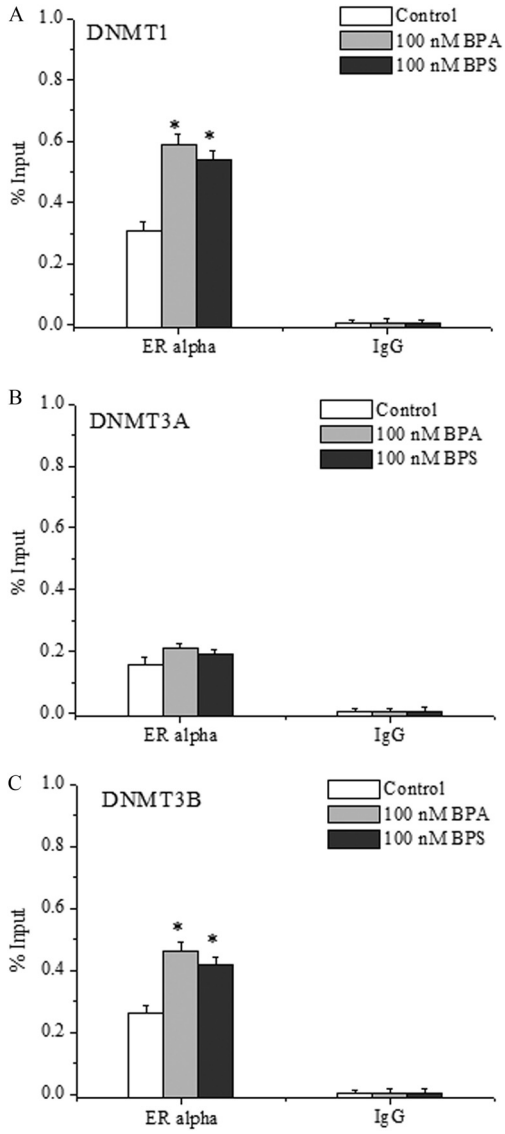

Figure 7. Chromatin immunoprecipitation–quantitative polymerase chain reaction (ChIP-qPCR) analysis of the binding of ERα to the promoters of (A) DNA methyltransferase (DNMT), (B) DNMT3A, and (C) DNMT3B genes in bisphenol A (BPA)- or bisphenol S (BPS)-treated MCF-7 cells. Data represent mean ± SD of three independent experiments. Statistical analysis was performed with Student's paired *t*-test, and asterisks indicate a significant difference from the control. *, $p < 0.05$. Note: SD, standard deviation.

upon BPA/BPS exposure (see Figure S10A–C). The depletion of ERα diminished the elevation of DNMT1 and DNMT3B induced by BPS/BPA exposure, at both the expression levels of mRNA and protein (see Figure S10D–F). However, the expression of DNMT3A in ERα$^{-/-}$ MCF-7 cells displayed a similar pattern as that in ERα$^{+/+}$ MCF-7 cells (see Figure S10D–F).

Furthermore, ChIP-qPCR analysis showed that the binding of ERα to the promoter regions of DNMT1 and DNMT3B was notably enhanced by BPA/BPS treatment (Figure 7A,C), whereas there was no significant difference in the binding of ERα to the promoter regions of DNMT3A (Figure 7B). ChIP-qPCR supported the enrichment of DNMT1, DNMT3A, and DNMT3B on TET2 promoter as induced by BPA/BPS treatment (Figure 8A).

To verify the regulatory effect of DNMT proteins on TET2 expression, vectors for shDNMT1, shDNMT3A, and shDNMT3B were constructed and transfected into MCF-7 cells. The transfection of DNMT1-shRNA, DNMT3A-shRNA, and DNMT3B-shRNA plasmids could reduce the protein expression of only the target genes (Figure 8B), and the knockdown of either DNMT1 or DNMT3A inhibited their proliferation (Figure 8C). Meanwhile, UHPLC-MS/MS analysis showed that the knockdown of both DNMT1 and DNMT3A partially alleviated the 5hmC decline induced by BPA/BPS exposure (Figure 8D). The TET2 expression in DNMT1- or DNMT3A-knockdown cells increased significantly at both transcriptional (Figure 8E) and protein levels (Figure 8F,G). Finally, the BSP sequencing-PCR showed that the methylation ratio of TET2 promoter induced by BPA/BPS exposure was decreased by knockdown of DNMT1, DNMT3A, or DNMT3B, especially for the knockdown of DNMT1 or DNMT3A (Figure 8H,I). Furthermore, using the second shRNA constructs for each DNMT gene for further confirmation resulted in similar results (see Figure S11).

Discussion

The results of the present study using an MCF-7 cell line suggest that the ubiquitous bisphenol pollutants BPA and BPS can repress both the expression of TET2 protein and its catalyzed DNA hydroxymethylation in ER$^+$ breast cancer cells. Environmentally relevant doses of BPA/BPS (Corrales et al. 2015), which also include measurable levels in body fluids and tissues (Vandenberg et al. 2007, 2010; Zhou et al. 2014), were used in this work, and our mechanistic study supports a tight linkage of these effects with the activation of ERα through dimerization and phosphorylation. Further exploration on the regulation by ERα on TET2 expression and DNA hydroxymethylation revealed a new feedback circuit of ERα activation–DNMT-TET2-DNA hydroxymethylation for shaping the proliferation of MCF-7 cells, which might be true for other ER$^+$ breast cancer cells. In this signal-transducing circuit, TET2 and its mediated DNA hydroxymethylation play a pivotal role in BPA/BPS-stimulated breast cancer cell proliferation.

TET2-Mediated DNA Hydroxymethylation Represses Bisphenol-Stimulated Proliferation

Widespread exposure to bisphenol compounds (BPA and BPS) of humans occurs through the oral, dermal, and inhalation routes. Low dosages of BPA/BPS might trigger a proliferative effect in various cell types, as has been shown for cells of the pancreatic islets (Carchia et al. 2015; Wei et al. 2017), endothelium (Xu et al. 2017), and breast after developmental treatment of mice with BPA (Acevedo et al. 2013) and cells of the pituitary gland of zebrafish treated with BPS (Ji et al. 2013) and a rat pituitary cell line after BPS treatment (Viñas and Watson 2013).

In this work, three breast cancer cell lines, MCF-7, T47D, and MDA-MB-231, were used in assaying proliferation. The first two cell lines are ER$^+$, and the last is triple-negative [ER/HER2/PR-negative (Veronesi et al. 2005)]. Notably, the MCF-7 cells had a higher ratio of ERα/ERβ than T47D cells (Lacroix and Leclercq 2004; Neve et al. 2006). Consistent with those reports, we also observed that BPA/BPS stimulated the proliferation of ER$^+$ breast cancer cells in a dose- and time-dependent manner (Figure 1; see also Figure S1).

Although bisphenol chemicals might have a function as a potential regulator of epigenetic modification (Acevedo et al. 2013; Manikkam et al. 2013; Singh and Li 2012) and BPA exposure has been shown to alter DNA methylation—BPA specifically increased DNA methylation of specific genes in the breast cancer epithelial cell line MCF-10 (Fernandez et al. 2012) and resulted in lower global methylation in the mouse placenta in an *in vivo* study (Susiarjo et al. 2013). The study of the effects of bisphenol chemicals on DNA hydroxymethylation has just begun (Kochmanski et al. 2018).

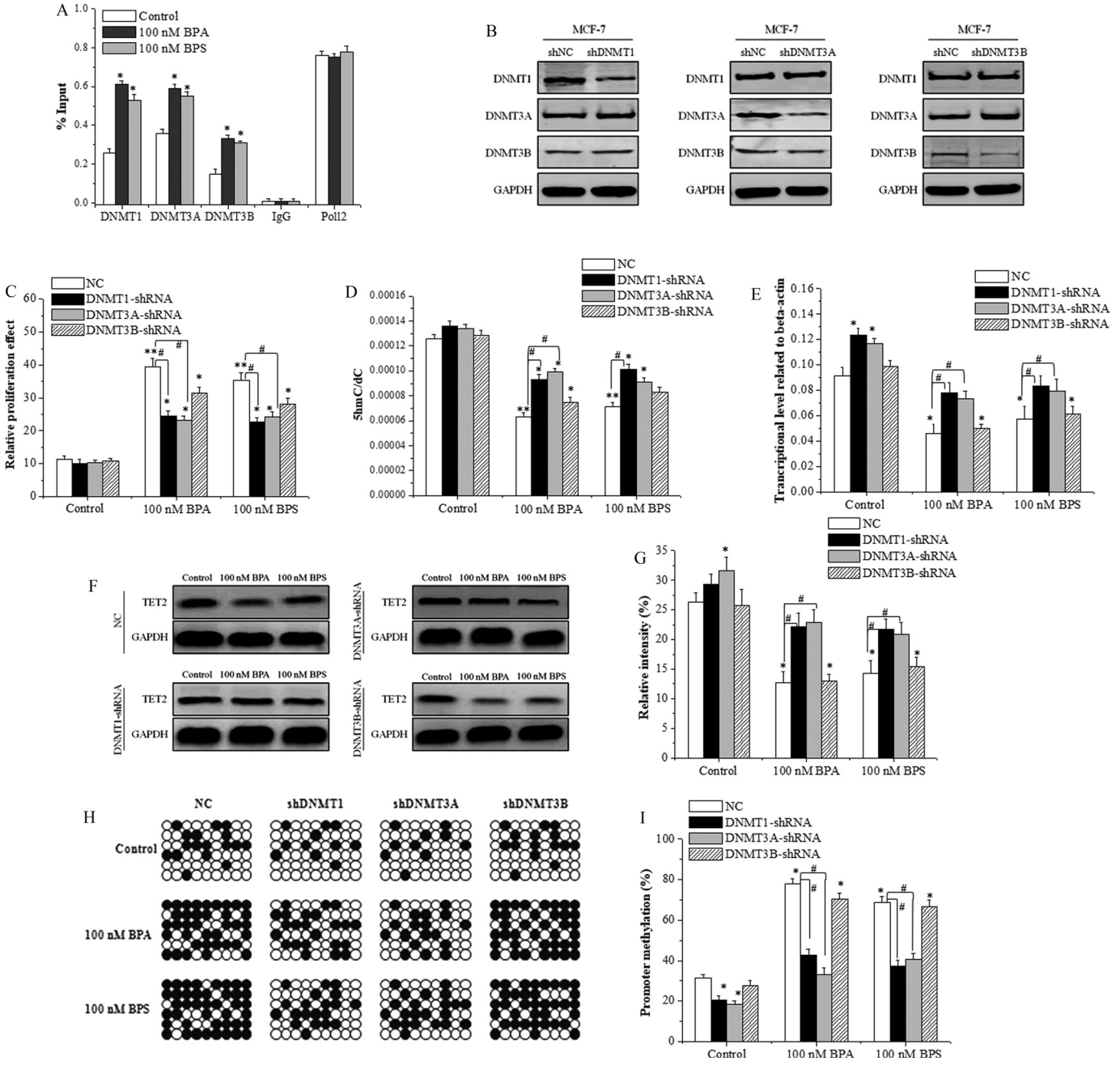

Figure 8. Regulation of ten-eleven translocation 2 (TET2) promoter methylation by DNA methyltransferases (DNMTs) in bisphenol A (BPA)- or bisphenol S (BPS)-treated MCF-7 cells. (A) Chromatin immunoprecipitation–quantitative polymerase chain reaction (ChIP-qPCR) analysis of the binding of DNMT1, DNMT3A, and DNMT3B to the promoter of the TET2 gene. Data represent mean ± SD of three independent experiments. Statistical analysis was performed with Student's paired *t*-test, and asterisks indicate a significant difference from the control. *, $p < 0.05$. (B) Identification of DNMT-knockdowns in the MCF-7 cells transfected with short hairpin RNA (shRNA)-DNMTs using Western blots. (C) MTS proliferation assay of MCF-7 cells transfected with shRNA-DNMTs in response to BPA/BPS treatment. Data represent mean ± SD of five independent experiments. (D) UHPLC-MS/MS analysis of 5hmC in genomic DNA of MCF-7 cells transfected with shRNA-DNMTs in response to BPA/BPS treatment. Data represent mean ± SD of five independent experiments. (E) qRT-PCR analysis of TET2 expression in MCF-7 cells transfected with shRNA-DNMTs at 48 h of BPA and BPS treatment. Data represent mean ± SD of five independent experiments. (F,G) Immunoblotting of TET2 protein in MCF-7 cells transfected with shRNA-DNMTs at 48 h of BPA and BPS treatment. The relative intensity was analyzed with ImageJ software (Schneider et al. 2012) and calculated by the ratio relative to the GAPDH intensity. Data represent mean ± SD of three independent experiments. (H,I) DNA sequencing analysis (H) and quantitative statistics (I) of methylation-specific PCR product of TET2 promoter in MCF-7 cells transfected with shRNA-DNMTs at 48 h of BPA/BPS treatment. Data represent mean ± SD of five independent experiments. Statistical significance was evaluated by two-way ANOVA (with Bonferroni posttest). *, $p < 0.05$ or **, $p < 0.01$ vs. control of cells transfected with shNC (NC); #, $p < 0.05$ vs. indicated samples. Note: ANOVA, analysis of variance; GAPDH, glyceraldehyde 3-phosphate dehydrogenase; MTS, a tetrazolium salt; SD, standard deviation; UHPLC-MRM MS/MS, ultra-high performance liquid chromatography–tandem mass spectrometry.

Here we showed that DMOG induced cell proliferation and 5hmC decline upon BPA/BPS exposure (Figure 1; Figure 3). Considering that DMOG is a potential competitor of α-KG in not only inhibiting the TET activity but also in inhibiting hypoxia inducible factor (HIF) prolyl hydroxylases and causing the stabilization of HIF1-alpha (Liu et al. 2009; Ghadge et al. 2017), inhibitory experiments alone cannot determine the vital roles of TET proteins in DNA hydroxymethylation and cell proliferation. Our study also

shows that TET2-mediated DNA hydroxymethylation plays a critical role in the proliferation of ER^+ breast cancer cells *in vitro*. Globally decreased 5hmC content was originally observed in hematological malignancies. Compared with normal tissues, a majority of cancers exhibited a global reduction in 5hmC, as observed in various regions of the genome, including in promoters (Jin et al. 2011; Jones 2012), gene bodies (Jones 2012), and intergenic regions (Feng and Fan 2009; Jones 2012). Similarly, in solid tumors such as melanoma, breast cancer, and prostate cancer, the loss of 5hmC and the dysregulation of TETs have been linked to malignant transformation and progression (Chou et al. 2011; Haffner et al. 2011; Jin et al. 2011; Tan and Shi 2012). Loss of 5hmC has been recognized as one of the key features of cancer, and DNA demethylation-mediated oncogene activation has been proposed to contribute to tumorigenesis (Jin et al. 2011; Ko et al. 2010). On the other hand, a large number of natural and synthetic chemicals have been reported to alter epigenetic DNA hydromethylation (Coulter et al. 2013; Heindel et al. 2015; Yin et al. 2013; Zhao et al. 2014). However, to our knowledge, no report has yet established a linkage between chemical exposure, DNA hydroxymethylation, and tumor-associated proliferation. Our data suggest that BPA/BPS exposure significantly decreases the genomic DNA 5hmC content in MCF-7 cells (Figure 3). The TET protein family, consisting of TET1, TET2, and TET3, is responsible for the formation of the 5hmC marker (Kohli and Zhang 2013). Hence, the decrease in 5hmC abundance can further be explained by the catalytic actions of the TET proteins (Ko et al. 2010; Kohli and Zhang 2013). We observed that the expression of TET2 at both the transcriptional and the protein levels was significantly higher than that of TET1 and TET3 in MCF-7 breast cancer cells (see Figure S2). The TET2 expression notably decreased upon BPA/BPS exposure (see Figure S2), and the depletion of TET2 remarkably promoted the BPA/BPS-induced proliferation of MCF-7 cells, whereas its overexpression inhibited the proliferation (Figure 4; see also Figures S3 and S4). Furthermore, use of the catalytic inhibitor DMOG showed that the inhibition on the catalytic activity of TET dioxygenases alone could repress the BPA/BPS-stimulated proliferation. Altogether, we have showed and corroborated the suppressive roles of TET2-mediated DNA hydroxymethylation in BPA/BPS-induced cell proliferation in MCF-7 cells.

Of note, we observed a reduced proliferation of MCF-7 cells treated with high doses of BPA, BPS, or E2. A high dose of estrogen-like compounds might activate the mitochondrial pathway of apoptosis (Li et al. 2019). Alternatively, by 72 h after BPA and BPS treatment, the excessive growth induced by BPA/BPS might result in insufficient nutrition within the culture medium in the 96-well plates, leading to inhibited proliferation.

Activation of ERα by BPA/BPS Modulates TET2-Mediated DNA Hydroxymethylation

Biochemical and genetic studies strongly suggest that an ER-dependent pathway implicated in gene transcriptional regulation underlies the mechanism of biological processes induced by bisphenol chemicals (Acconcia et al. 2015; Viñas and Watson 2013; La Rosa et al. 2014; Xu et al. 2014). ERs play vital roles in the classification, diagnosis, and treatment of breast cancer (Schneider et al. 2006). Phosphorylation of ERα/ERβ promotes the activation of intracellular signaling pathways that modulate gene transcription (Burns et al. 2011; Métivier et al. 2003; Pettersson and Gustafsson 2001). Our data show that BPA/BPS increased the phosphorylation of ERα (S118 and S167) but not ERβ (S87 and S105) in MCF-7 cells (see Figure S5). The toxicological effects of BPA and BPS are associated with their ability to regulate the actions of ERα and ERβ (Acconcia et al. 2015; Viñas and Watson 2013). In our work, the depletion of ERα, but not ERβ, diminished the BPA/BPS-stimulated proliferation that accompanied an elevation of TET2 expression, leading to an increase in genomic DNA hydroxymethylation (Figure 5). The knockdown of TET2 in $ER\alpha^{-/-}$ MCF-7 cells partly alleviated the inhibition on BPA/BPS-stimulated cell proliferation via reduced DNA hydroxymethylation (Figure 5). These results support that the activation of ERα represses TET2 expression and reduces genomic DNA hydroxymethylation. In this pathway, BPA/BPS exposure is a key initiating event for the activation of ERα and the inhibition of TET2-mediated DNA hydroxymethylation. On the other hand, TET2 plays a pivotal role in repressing bisphenol-stimulated breast cancer cell proliferation.

ERα Enhances DNMT-Mediated Promoter Methylation of TET2

Most CpG-rich regions (CpG islands) overlap with proximal promoters, whereas DNA methylation is linked to gene silencing (Wu and Zhang 2014). It should be noted that the TET2 gene possesses a CpG island in the promoter region. Regarding undetectable interaction between ERα and TET2 protein (Figure 6), we focused on the

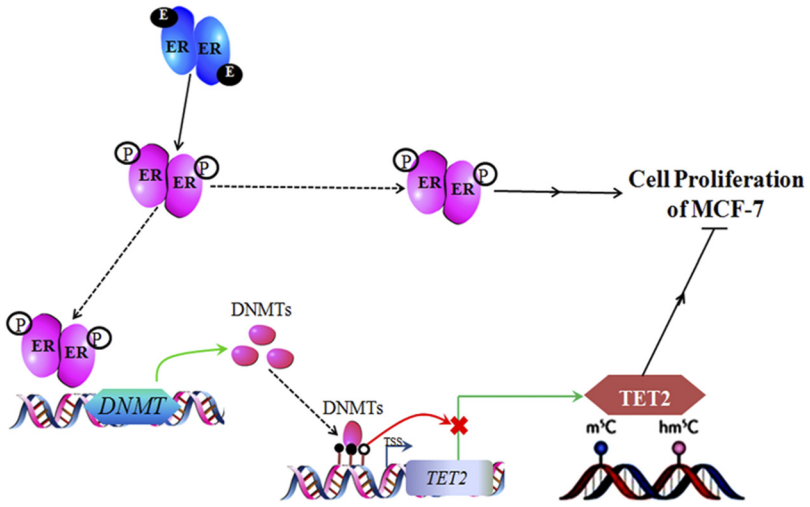

Figure 9. Proposed ERα-DNA methyltransferase (DNMT)–ten-eleven translocation 2 (TET2) pathway for modulating bisphenol A (BPA)- or bisphenol S (BPS)-stimulated proliferation in $ER\alpha^+$ breast cancer cells. Note: E, estrogen; ER, estrogen receptor; hm^5C, DNA 5-hydroxymethylcytosine; m^5C, DNA 5-methylcytosine m5C; P, phosphorylation.

possible involvement of the promoter methylation of the TET2 gene. The methylation of CpG islands in the promoter region of genes is a well-known inhibitory mechanism for down-regulation of gene and protein expression (Figueroa et al. 2010; Gong et al. 2017). The hypermethylation of TET1 gene has been found in multiple primary tumors (Li et al. 2016), and DNMT3A-mediated methylation of TET2 and TET3 promoters has been implicated in the induction of the epithelial–mesenchymal transition-like process and metastasis in melanoma (Gong et al. 2017). TET2 promoter methylation has been implicated in lymphoblastic leukemia (Figueroa et al. 2010; Musialik et al. 2014) and has also been reported in a small fraction (4.4%) of myeloproliferative neoplasms (Chim et al. 2010). We showed that in an ERα-dependent manner, TET2 promoter methylation was elevated by BPA/BPS exposure (Figure 6). Accumulating evidence supports that, in a number of human malignancies, DNMTs mediate transcriptional silencing, which is characterized by DNA hypermethylation of promoter regions (Foltz et al. 2009; Jones 2012; Wu et al. 2010; Wu and Zhang 2014). Our ChIP-qPCR data show that the increased binding of DNMT1, DNMT2, and DNMT3B to the TET2 promoter induced by BPA/BPS treatment and the knockdown of DNMT1 and DNMT3B effectively diminishes the promoter methylation of TET2 and up-regulates TET2 expression, resulting in an increase in DNA hydroxymethylation accompanied by an inhibition of the BPA/BPS-stimulated proliferation of MCF-7 cells (Figure 8; see also Figure S11).

It should be mentioned that we detected the promoter methylation of TET2 using bisulfite sequencing, which cannot distinguish 5hmC from 5mC (Huang et al. 2010). Hence, the data of the TET2 promoter methylation level might be affected by the existence of 5hmC. However, the content of 5hmC is much lower than that of 5mC in genomic DNA (Branco et al. 2011; Shen and Zhang 2013).

Furthermore, ERα was found to be critical for the increased expression of DNMT1 and DNMT3A induced by BPA/BPS, whereas ChIP-qPCR data indicate that a direct interaction of ERα with the promoter regions of DNMT1 and DNMT3B, but not DNMT3A, was notably enhanced by BPA/BPS treatment (Figure 7). These results indicated that ERα induced epigenetic silence of TET2 by DNMT-catalyzed promoter methylation in the BPA/BPS-treated MCF-7 proliferation. Interestingly, DNMT3A was involved in the modulation of TET2 expression, but was not directly regulated by ERα, implying the complexity and diversity of the signal pathways involved in the regulation of the biological processes induced by BPA/BPS in MCF-7 cells.

Proposed ERα-DNMT-TET2 Pathway

Based on our data and the above discussion, we propose a signal transduction feedback pathway for ER^+ breast cells (Figure 9): TET2 and its mediated DNA hydroxymethylation restrict the proliferation. Upon binding of BPA/BPS to ERα, an ERα homodimer forms and is further phosphorylated, leading to ERα activation. The activated ERα homodimer translocates into the nucleus to bind to the promoter region of the DNMT genes (DNMT1 and DNMT3B) to promote their transcription, which is followed by increased translation. The binding of the increased DNMT proteins to the promoter region of TET2 elevates the methylation of its CpG island. With the elevated methylation, both the transcription and expression of TET2 gene are repressed, reducing genomic 5hmC, ultimately promoting the proliferation of breast cancer cells.

In summary, our study revealed a regulatory mechanism of ERα on TET2 protein and uncovered a signal-transducing circuit of ERα–DNMT1/3B-TET2-DNA hydroxymethylation for shaping the proliferation of MCF-7 cells. This might be also true for other ER^+ breast cancer cells. The bisphenol chemical exposure functions as an initiator for all these biological events. Our study revealed new insight into the toxicology and pathogenic effects of bisphenol chemicals, emphasizing the pathway of ER receptor–DNMTs-TET2-DNA hydroxymethylation.

Acknowledgments

This study was supported by grants from the National Science Foundation of China (21607169, 91743201, and 21621064), the Ministry of Science and Technology of China (2018YFC1005003), the Key Research Program of Frontier Sciences, Chinese Academy of Sciences (QYZDJ-SSW-DQC017), the K.C. Wong Education Foundation, and Sanming Project of Medicine in Shenzhen (SZM201811070).

References

Acconcia F, Pallottini V, Marino M. 2015. Molecular mechanisms of action of BPA. Dose Response 13(4):1559325815610582, PMID: 26740804, https://doi.org/10.1177/1559325815610582.

Acevedo N, Davis B, Schaeberle CM, Sonnenschein C, Soto AM. 2013. Perinatally administered bisphenol A as a potential mammary gland carcinogen in rats. Environ Health Perspect 121(9):1040–1046, PMID: 23876597, https://doi.org/10.1289/ehp.1306734.

Albano F, Anelli L, Zagaria A, Coccaro N, Minervini A, Rossi AR, et al. 2011. Decreased *TET2* gene expression during chronic myeloid leukemia progression. Leuk Res 35(11):e220–e222, PMID: 21794915, https://doi.org/10.1016/j.leukres.2011.07.013.

Aungst J. 2014. Division of Food Contact Notifications, Office of Food Additive Safety (OFAS), Center for Food Safety and Applied Nutrition (CFSAN, HFS-275), to M Landa, Director, CFSAN (HFS-001). 2014 updated safety assessment of bisphenol A (BPA) for use in food contact applications. https://www.fda.gov/downloads/newsevents/publichealthfocus/ucm424266.pdf [accessed 11 February 2020].

Branco MR, Ficz G, Reik W. 2011. Uncovering the role of 5-hydroxymethylcytosine in the epigenome. Nat Rev Genet 13(1):7–13, PMID: 22083101, https://doi.org/10.1038/nrg3080.

Burns KA, Li Y, Arao Y, Petrovich RM, Korach KS. 2011. Selective mutations in estrogen receptor α D-domain alters nuclear translocation and non-estrogen response element gene regulatory mechanisms. J Biol Chem 286(14):12640–12649, PMID: 21285458, https://doi.org/10.1074/jbc.M110.187773.

Calafat AM, Kuklenyik Z, Reidy JA, Caudill SP, Ekong J, Needham LL. 2005. Urinary concentrations of bisphenol A and 4-nonylphenol in a human reference population. Environ Health Perspect 113(4):391–395, PMID: 15811827, https://doi.org/10.1289/ehp.7534.

Carchia E, Porreca I, Almeida PJ, D'Angelo F, Cuomo D, Ceccarelli M, et al. 2015. Evaluation of low doses BPA-induced perturbation of glycemia by toxicogenomics points to a primary role of pancreatic islets and to the mechanism of toxicity. Cell Death Dis 6:e1959, PMID: 26512966, https://doi.org/10.1038/cddis.2015.319.

Chen D, Kannan K, Tan H, Zheng Z, Feng YL, Wu Y, et al. 2016. Bisphenol analogues other than BPA: environmental occurrence, human exposure, and toxicity—a review. Environ Sci Technol 50(11):5438–5453, PMID: 27143250, https://doi.org/10.1021/acs.est.5b05387.

Chim CS, Wan TS, Fung TK, Wong KF. 2010. Methylation of TET2, CBL and CEBPA in Ph-negative myeloproliferative neoplasms. J Clin Pathol 63(10):942–946, PMID: 20671051, https://doi.org/10.1136/jcp.2010.080218.

Chou WC, Chou SC, Liu CY, Chen CY, Hou HA, Kuo YY, et al. 2011. *TET2* mutation is an unfavorable prognostic factor in acute myeloid leukemia patients with intermediate-risk cytogenetics. Blood 118(14):3803–3810, PMID: 21828143, https://doi.org/10.1182/blood-2011-02-339747.

Corrales J, Kristofco LA, Steele WB, Yates BS, Breed CS, Williams ES, et al. 2015. Global assessment of bisphenol A in the environment: review and analysis of its occurrence and bioaccumulation. Dose Response 13(3):1559325815598308, PMID: 26674671, https://doi.org/10.1177/1559325815598308.

Coulter JB, O'Driscoll CM, Bressler JP. 2013. Hydroquinone increases 5-hydroxymethylcytosine formation through ten eleven translocation 1 (TET1) 5-methylcytosine dioxygenase. J Biol Chem 288(40):28792–28800, PMID: 23940045, https://doi.org/10.1074/jbc.M113.491365.

EFSA CEF Panel (European Food Safety Authority Panel on Food Contact Materials, Enzymes, Flavourings and Processing Aids). 2015. Scientific opinion on the risks to public health related to the presence of bisphenol A (BPA) in food stuffs: executive summary. EFSA J 13(1):3978, https://doi.org/10.2903/j.efsa.2015.3978.

Feng J, Fan G. 2009. The role of DNA methylation in the central nervous system and neuropsychiatric disorders. Int Rev Neurobiol 89:67–84, PMID: 19900616, https://doi.org/10.1016/S0074-7742(09)89004-1.

Fernandez SV, Huang Y, Snider KE, Zhou Y, Pogash TJ, Russo J. 2012. Expression and DNA methylation changes in human breast epithelial cells after bisphenol A exposure. Int J Oncol 41(1):369–377, PMID: 22576693, https://doi.org/10.3892/ijo.2012.1444.

Ficz G, Branco MR, Seisenberger S, Santos F, Krueger F, Hore TA, et al. 2011. Dynamic regulation of 5-hydroxymethylcytosine in mouse ES cells and during differentiation. Nature 473(7347):398–402, PMID: 21460836, https://doi.org/10.1038/nature10008.

Figueroa ME, Abdel-Wahab O, Lu C, Ward PS, Patel J, Shih A, et al. 2010. Leukemic IDH1 and IDH2 mutations result in a hypermethylation phenotype, disrupt TET2 function, and impair hematopoietic differentiation. Cancer Cell 18(6):553–567, PMID: 21130701, https://doi.org/10.1016/j.ccr.2010.11.015.

Foltz G, Yoon JG, Lee H, Ryken TC, Sibenaller Z, Ehrich M, et al. 2009. DNA methyltransferase-mediated transcriptional silencing in malignant glioma: a combined whole-genome microarray and promoter array analysis. Oncogene 28(29):2667–2677, PMID: 19465937, https://doi.org/10.1038/onc.2009.122.

Ghadge SK, Messner M, Van Pham T, Doppelhammer M, Petry A, Görlach A, et al. 2017. Prolyl-hydroxylase inhibition induces SDF-1 associated with increased CXCR4+/CD11b+ subpopulations and cardiac repair. J Mol Med (Berl) 95(8):825–837, PMID: 28550361, https://doi.org/10.1007/s00109-017-1543-3.

Gong F, Guo Y, Niu Y, Jin J, Zhang X, Shi X, et al. 2017. Epigenetic silencing of TET2 and TET3 induces an EMT-like process in melanoma. Oncotarget 8(1):315–328, PMID: 27852070, https://doi.org/10.18632/oncotarget.13324.

Haffner MC, Chaux A, Meeker AK, Esopi DM, Gerber J, Pellakuru LG, et al. 2011. Global 5-hydroxymethylcytosine content is significantly reduced in tissue stem/progenitor cell compartments and in human cancers. Oncotarget 2(8):627–637, PMID: 21896958, https://doi.org/10.18632/oncotarget.316.

He YF, Li BZ, Li Z, Liu P, Wang Y, Tang Q, et al. 2011. Tet-mediated formation of 5-carboxylcytosine and its excision by TDG in mammalian DNA. Science 333(6047):1303–1307, PMID: 21817016, https://doi.org/10.1126/science.1210944.

Heindel JJ, Balbus J, Birnbaum L, Brune-Drisse MN, Grandjean P, Gray K, et al. 2015. Developmental origins of health and disease: integrating environmental influences. Endocrinology 156(10):3416–3421, PMID: 26241070, https://doi.org/10.1210/EN.2015-1394.

Héliès-Toussaint C, Peyre L, Costanzo C, Chagnon MC, Rahmani R. 2014. Is bisphenol S a safe substitute for bisphenol A in terms of metabolic function? An *in vitro* study. Toxicol Appl Pharmacol 280(2):224–235, PMID: 25111128, https://doi.org/10.1016/j.taap.2014.07.025.

Huang Y, Pastor WA, Shen Y, Tahiliani M, Liu DR, Rao A. 2010. The behaviour of 5-hydroxymethylcytosine in bisulfite sequencing. PLoS One 5(1):e8888, PMID: 20126651, https://doi.org/10.1371/journal.pone.0008888.

Ji K, Hong S, Kho Y, Choi K. 2013. Effects of bisphenol S exposure on endocrine functions and reproduction of zebrafish. Environ Sci Technol 47(15):8793–8800, PMID: 23806087, https://doi.org/10.1021/es400329t.

Jin SG, Jiang Y, Qiu R, Rauch TA, Wang Y, Schackert G, et al. 2011. 5-Hydroxymethylcytosine is strongly depleted in human cancers but its levels do not correlate with *IDH1* mutation. Cancer Res 71(24):7360–7365, PMID: 22052461, https://doi.org/10.1158/0008-5472.CAN-11-2023.

Jones PA. 2012. Functions of DNA methylation: islands, start sites, gene bodies and beyond. Nat Rev Genet 13(7):484–492, PMID: 22641018, https://doi.org/10.1038/nrg3230.

Kinch CD, Ibhazehiebo K, Jeong JH, Habibi HR, Kurrasch DM. 2015. Low-dose exposure to bisphenol A and replacement bisphenol S induces precocious hypothalamic neurogenesis in embryonic zebrafish. Proc Natl Acad Sci USA 112(5):1475–1480, PMID: 25583509, https://doi.org/10.1073/pnas.1417731112.

Ko M, Huang Y, Jankowska AM, Pape UJ, Tahiliani M, Bandukwala HS, et al. 2010. Impaired hydroxylation of 5-methylcytosine in myeloid cancers with mutant *TET2*. Nature 468(7325):839–843, PMID: 21057493, https://doi.org/10.1038/nature09586.

Kochmanski JJ, Marchlewicz EH, Cavalcante RG, Perera BPU, Sartor MA, Dolinoy DC. 2018. Longitudinal effects of developmental bisphenol A exposure on epigenome-wide DNA hydroxymethylation at imprinted loci in mouse blood. Environ Health Perspect 126(7):077006, PMID: 30044229, https://doi.org/10.1289/EHP3441.

Kohli RM, Zhang Y. 2013. TET enzymes, TDG and the dynamics of DNA demethylation. Nature 502(7472):472–479, PMID: 24153300, https://doi.org/10.1038/nature12750.

La Rosa P, Pellegrini M, Totta P, Acconcia F, Marino M. 2014. Xenoestrogens alter estrogen receptor (ER) α intracellular levels. PLoS One 9(2):e88961, PMID: 24586459, https://doi.org/10.1371/journal.pone.0088961.

Lacroix M, Leclercq G. 2004. Relevance of breast cancer cell lines as models for breast tumours: an update. Breast Cancer Res Treat 83(3):249–289, PMID: 14758095, https://doi.org/10.1023/B:BREA.0000014042.54925.cc.

Li D, Chen J, Ai Y, Gu X, Li L, Che D, et al. 2019. Estrogen-related hormones induce apoptosis by stabilizing Schlafen-12 protein turnover. Mol Cell 75(6):1103–1116.e9, PMID: 31420216, https://doi.org/10.1016/j.molcel.2019.06.040.

Li L, Li C, Mao H, Du Z, Chan WY, Murray P, et al. 2016. Epigenetic inactivation of the CpG demethylase TET1 as a DNA methylation feedback loop in human cancers. Sci Rep 6:26591, PMID: 27225590, https://doi.org/10.1038/srep26591.

Liao CY, Liu F, Alomirah H, Loi VD, Mohd MA, Moon HB, et al. 2012. Bisphenol S in urine from the United States and seven Asian countries: occurrence and human exposures. Environ Sci Technol 46(12):6860–6866, PMID: 22620267, https://doi.org/10.1021/es301334j.

Liu J, Jiang J, Mo J, Liu D, Cao D, Wang H, et al. 2019. Global DNA 5-hydroxymethylcytosine and 5-formylcytosine contents are decreased in the early stage of hepatocellular carcinom. Hepatology 69(1):196–208, PMID: 30070373, https://doi.org/10.1002/hep.30146.

Liu XB, Wang JA, Ogle ME, Wei L. 2009. Prolyl hydroxylase inhibitor dimethyloxalylglycine enhances mesenchymal stem cell survival. J Cell Biochem 106(5):903–911, PMID: 19229863, https://doi.org/10.1002/jcb.22064.

López-Sáez JF, de la Torre C, Pincheira J, Giménez-Martín G. 1998. Cell proliferation and cancer. Histo Histopathol 13(4):1197–1214, PMID: 9810511, https://doi.org/10.14670/HH-13.1197.

Malich G, Markovic B, Winder C. 1997. The sensitivity and specificity of the MTS tetrazolium assay for detecting the *in vitro* cytotoxicity of 20 chemicals using human cell lines. Toxicology 124(3):179–192, PMID: 9482120, https://doi.org/10.1016/S0300-483X(97)00151-0.

Manikkam M, Tracey R, Guerrero-Bosagna C, Skinner MK. 2013. Plastics derived endocrine disruptors (BPA, DEHP and DBP) induce epigenetic transgenerational inheritance of obesity, reproductive disease and sperm epimutations. PLoS One 8(1):e55387, PMID: 23359474, https://doi.org/10.1371/journal.pone.0055387.

Métivier R, Penot G, Hübner MR, Reid G, Brand H, Kos M, et al. 2003. Estrogen receptor-α directs ordered, cyclical, and combinatorial recruitment of cofactors on a natural target promoter. Cell 115(6):751–763, PMID: 14675539, https://doi.org/10.1016/S0092-8674(03)00934-6.

Michałowicz J. 2014. Bisphenol A—sources, toxicity and biotransformation. Environ Toxicol Pharmacol 37(2):738–758, PMID: 24632011, https://doi.org/10.1016/j.etap.2014.02.003.

Musialik E, Bujko M, Wypych A, Matysiak M, Siedlecki JA. 2014. TET2 promoter DNA methylation and expression analysis in pediatric B-cell acute lymphoblastic leukemia. Hematol Rep 6(1):5333, PMID: 24711921, https://doi.org/10.4081/hr.2014.5333.

Neve RM, Chin K, Fridlyand J, Yeh J, Baehner FL, Fevr T, et al. 2006. A collection of breast cancer cell lines for the study of functionally distinct cancer subtypes. Cancer Cell 10(6):515–527, PMID: 17157791, https://doi.org/10.1016/j.ccr.2006.10.008.

Pettersson K, Gustafsson JÅ. 2001. Role of estrogen receptor beta in estrogen action. Annu Rev Physiol 63:165–192, PMID: 11181953, https://doi.org/10.1146/annurev.physiol.63.1.165.

Pfeifer D, Chung YM, Hu MCT. 2015. Effects of low-dose bisphenol A on DNA damage and proliferation of breast cells: the role of c-Myc. Environ Health Perspect 123(12):1271–1279, PMID: 25933419, https://doi.org/10.1289/ehp.1409199.

Rochester JR, Bolden AL. 2015. Bisphenol S and F: a systematic review and comparison of the hormonal activity of bisphenol A substitutes. Environ Health Perspect 123(7):643–650, PMID: 25775505, https://doi.org/10.1289/ehp.1408989.

Rodgers KM, Udesky JO, Rudel RA, Brody JG. 2018. Environmental chemicals and breast cancer: an updated review of epidemiological literature informed by biological mechanisms. Environ Res 160:152–182, PMID: 28987728, https://doi.org/10.1016/j.envres.2017.08.045.

Schneider CA, Rasband WS, Eliceiri KW. 2012. NIH Image to ImageJ: 25 years of image analysis. Nat Methods 9(7):671–675, PMID: 22930834, https://doi.org/10.1038/nmeth.2089.

Schneider J, Ruschhaupt M, Buness A, Asslaber M, Regitnig P, Zatloukal K, et al. 2006. Identification and meta-analysis of a small gene expression signature for the diagnosis of estrogen receptor status in invasive ductal breast cancer. Int J Cancer 119(12):2974–2979, PMID: 17019712, https://doi.org/10.1002/ijc.22234.

Shen L, Zhang Y. 2013. 5-Hydroxymethylcytosine: generation, fate, and genomic distribution. Curr Opin Cell Biol 25(3):289–296, PMID: 23498661, https://doi.org/10.1016/j.ceb.2013.02.017.

Singh S, Li SS. 2012. Epigenetic effects of environmental chemicals bisphenol A and phthalates. Int J Mol Sci 13(8):10143–10153, PMID: 22949852, https://doi.org/10.3390/ijms130810143.

Susiarjo M, Sasson I, Mesaros C, Bartolomei MS. 2013. Bisphenol A exposure disrupts genomic imprinting in the mouse. PLoS Genet 9(4):e1003401, PMID: 23593014, https://doi.org/10.1371/journal.pgen.1003401.

Tahiliani M, Koh KP, Shen Y, Pastor WA, Bandukwala H, Brudno Y, et al. 2009. Conversion of 5-methylcytosine to 5-hydroxymethylcytosine in mammalian DNA by MLL partner TET1. Science 324(5929):930–935, PMID: 19372391, https://doi.org/10.1126/science.1170116.

Tan L, Shi YG. 2012. Tet family proteins and 5-hydroxymethylcytosine in development and disease. Development 139(11):1895–1902, PMID: 22569552, https://doi.org/10.1242/dev.070771.

Vandenberg LN, Chahoud I, Heindel JJ, Padmanabhan V, Paumgartten FJ, Schoenfelder G. 2010. Urinary, circulating, and tissue biomonitoring studies

indicate widespread exposure to bisphenol A. Environ Health Perspect 118(8):1055–1070, PMID: 20338858, https://doi.org/10.1289/ehp.0901716.
Vandenberg LN, Hauser R, Marcus M, Olea N, Welshons WV. 2007. Human exposure to bisphenol A (BPA). Reprod Toxicol 24(2):139–177, PMID: 17825522, https://doi.org/10.1016/j.reprotox.2007.07.010.
Veronesi U, Boyle P, Goldhirsch A, Orecchia R, Viale G. 2005. Breast cancer. Lancet 365(9472):1727–1741, PMID: 15894099, https://doi.org/10.1016/S0140-6736(05)66546-4.
Viñas R, Watson CS. 2013. Bisphenol S disrupts estradiol-induced nongenomic signaling in a rat pituitary cell line: effects on cell functions. Environ Health Perspect 121(3):352–358, PMID: 23458715, https://doi.org/10.1289/ehp.1205826.
Wei J, Ding D, Wang T, Liu Q, Lin Y. 2017. MiR-338 controls BPA-triggered pancreatic islet insulin secretory dysfunction from compensation to decompensation by targeting Pdx-1. FASEB J 31(12):5184–5195, PMID: 28774890, https://doi.org/10.1096/fj.201700282R.
Wu H, Coskun V, Tao J, Xie W, Ge W, Yoshikawa K, et al. 2010. Dnmt3a-dependent nonpromoter DNA methylation facilitates transcription of neurogenic genes. Science 329(5990):444–448, PMID: 20651149, https://doi.org/10.1126/science.1190485.
Wu H, Zhang Y. 2014. Reversing DNA methylation: mechanisms, genomics, and biological functions. Cell 156(1–2):41–68, PMID: 24439369, https://doi.org/10.1016/j.cell.2013.12.019.
Wu SC, Zhang Y. 2010. Active DNA demethylation: many roads lead to Rome. Nat Rev Mol Cell Biol 11(9):607–620, PMID: 20683471, https://doi.org/10.1038/nrm2950.
Xu F, Wang X, Wu N, He S, Yi W, Xiang S, et al. 2017. Bisphenol A induces proliferative effects on both breast cancer cells and vascular endothelial cells through a shared GPER-dependent pathway in hypoxia. Environ Pollut 231(Pt 2):1609–1620, PMID: 28964603, https://doi.org/10.1016/j.envpol.2017.09.069.
Xu XB, He Y, Song C, Ke X, Fan SJ, Peng WJ, et al. 2014. Bisphenol A regulates the estrogen receptor alpha signaling in developing hippocampus of male rats through estrogen receptor. Hippocampus 24(12):1570–1580, PMID: 25074486, https://doi.org/10.1002/hipo.22336.
Yin RC, Mao S-Q, Zhao BL, Chong Z, Yang Y, Zhao C, et al. 2013. Ascorbic acid enhances Tet-mediated 5-methylcytosine oxidation and promotes DNA demethylation in mammals. J Am Chem Soc 135(28):10396–10403, PMID: 23768208, https://doi.org/10.1021/ja4028346.
Zhang ZF, Alomirah H, Cho HS, Li YF, Liao CY, Minh TB, et al. 2011. Urinary bisphenol A concentrations and their implications for human exposure in several Asian countries. Environ Sci Technol 45(16):7044–7050, PMID: 21732633, https://doi.org/10.1021/es200976k.
Zhao BL, Yang Y, Wang XL, Chong ZC, Yin RC, Song SH, et al. 2014. Redox-active quinones induces genome-wide DNA methylation changes by an iron-mediated and Tet-dependent mechanism. Nucleic Acids Res 42(3):1593–1605, PMID: 24214992, https://doi.org/10.1093/nar/gkt1090.
Zhong S, Li C, Han X, Li X, Yang YG, Wang H. 2019. Idarubicin stimulates cell cycle- and TET2-dependent oxidation of DNA 5-methylcytosine in cancer cells. Chem Res Toxicol 32(5):861–868, PMID: 30816036, https://doi.org/10.1021/acs.chemrestox.9b00012.
Zhou X, Kramer JP, Calafat AM, Ye X. 2014. Automated on-line column-switching high performance liquid chromatography isotope dilution tandem mass spectrometry method for the quantification of bisphenol A, bisphenol F, bisphenol S, and 11 other phenols in urine. J Chromatogr B Analyt Technol Biomed Life Sci 944:152–156, PMID: 24316527, https://doi.org/10.1016/j.jchromb.2013.11.009.
Zhu J, Thompson CB. 2019. Metabolic regulation of cell growth and proliferation. Nat Rev Mol Cell Biol 20(7):436–450, PMID: 30976106, https://doi.org/10.1038/s41580-019-0123-5.